Design methodology of ship structure based on optimization algorithm

（最適化アルゴリズムに基づく船舶構造設計法）

Sep. 2018

LIU ZHIJUN

ABSTRACT

Design methodology of ship structure based on optimization algorithm

As the development of technology and globalization economic, the competition in the shipbuilding industry is becoming more and more intense. So, designing sophisticate ship structures that satisfy several design criteria simultaneously with minimum weight and cost is an important engineering issue. Structural optimization technology has developed rapidly in recent years and are widely applied in various industries. in this thesis, a series of optimization methods are applied to optimize the ship structures,

There are two ship structure are set as optimization object in this thesis, which are talk in the follow,

one research object is ship prow, the purpose for this object is to obtain the optimal stiffeners location and its size. Firstly, adopting the topology optimization with some manufacturing constraints to predict the possible stiffener location, and arrange the T style stiffener to replace the potential stiffener on the plate based on topology optimization results and engineering experience; later five design variables are selected, the value of variation range and the parameter relationships among these five design variables are determined for avoid producing invalid dimensions. and adopting size optimization method to optimize the stiffener size and plate thickness based on the above stiffeners;

The other research object is radar mast, the purpose for this object is to minimize its weight within the eigen frequency. the integration shape and size optimization method

is adopted for radar mast, an approximate shape and size results can be obtained, but its curve surface does not change uniformly, it is hard to manufacture. Then we construct a new model based on the above optimization results for saving subsequent optimization time. And apply the integration optimization method to optimize the curvilinear equation and plate thickness of new model, getting a reasonable radar mast. These results prove that structure optimization technology is helpful to design new ship and shorten the design cycle.

Acknowledge

internship, they also provided me numerous invaluable comments, ideas for the co-research project.

Finally, I'd like to express my deepest appreciation to my parents, sister and brother, brother for their warm encouragements and financial support, making me more determined and persevered to finish my career as a student. In the future, I will work harder to repay their care.

Contents

List of tables

List of figures

Main symbols

ρ ⋯⋯⋯⋯ Material density

V ⋯⋯⋯⋯ Volume of the initial design domain

E ⋯⋯⋯⋯ Material elasticity modulus

p ⋯⋯⋯⋯ Penalty factors

k ⋯⋯⋯⋯ Bulk modulus

μ ⋯⋯⋯⋯ Shear modulus

v ⋯⋯⋯⋯ Poisson's ratio

C ⋯⋯⋯⋯ Structure compliance

U ⋯⋯⋯⋯ Displacement matrix

K ⋯⋯⋯⋯ Stiffness matrix

f ⋯⋯⋯⋯ Volume ratio

P ⋯⋯⋯⋯ Hydrostatic pressure

f_0 ⋯⋯⋯⋯ Given frequency

σ_{max} ⋯⋯⋯⋯ Maximum stress

t ⋯⋯⋯⋯ Thickness

$[\sigma]$ ⋯⋯⋯⋯ Allowable stress

M ⋯⋯⋯⋯ Structure weight

ω_i ⋯⋯⋯⋯ i-th order frequency

Chapter 1

Introduction

1.1 Research Background

Shipbuilding companies are confronting new opportunities and challenges with the development of technology and economy. In particular, the public is increasingly concerned about the environmental problems caused by shipping activities such as the depletion of oil resources and environmental pollution, political and business and leaders have extensively talk about the environmental protection and resource conservation[1]. And the international maritime organization also issues various regulations and convention to solve the above problem, protect the whole biological environment effectively and require the ship industry to follow the concept of green environmental protection. Therefore, the green shipbuilding follows the low emission, low fuel consumption, energy saving and environmental protection become the inevitable trend of shipbuilding industry in the future. To achieve the above requirements, reducing weight is the most important measure.

Optimization techniques are powerful tools for improving traditional structural designs in many real applications, particularly in aerospace and marine engineering. A remarkable phenomenon seen in recent years has been the rapid growth of theoretical studies and practical applications of topology, shape and size optimization for conceptual and detailed design in structural optimization[2-5]. Such as, Lei adopted the topology technology to design the head of a new pure electric bus, at the same time, combining the orthogonal design with structural finite element method, and considering the safety of collision, the goal of lightweight and optimal energy

absorption is achieved[6]. Hu used topology optimization and size optimization to optimize the torsional stiffness of the body as the optimization target, based on the first order torsional frequency, which makes the body's torsional stiffness significantly improved[7]. with the development of topology optimization technology, this technology has also been applied in the additive manufacturing. Matthew combines the topology optimization technology and the additive manufacturing technology to redesign and manufacture the engine room bracket of the aircraft, the weight and stress of the scaffold were reduced by 64% and 50% respectively[8]. Wang used the topology optimization and additive manufacturing technology to optimize the truss in skin frame, and a better mechanical performance is obtained[9]. Optimization technology is also often applied in shipbuilding industry. D.Kavlie and J.Moe used mathematical programming method for the first time in the application of ship structure design, thus opening up the age of ship structure design[10]. for example, the application in the design of stiffeners, the structure of plate with stiffeners is being widely applying in automotive, aerospace and other industry filed, because this structure not only can reduce weight, but also has higher mechanical performance, such as stiffness, strength, and so on. it's known that there are many shell structures in hull parts, these shell structures need to be strengthened by stiffener, the stiffener weight accounted for about 30% of the total hull weight [11], so we should arrange the stiffener layout reasonably with suitable size to reduce stiffener weight, which not only improve the structural mechanical performance, but also can reduce shipbuilding cost (including the raw material and labor fee) and improve competitiveness in shipbuilding industry. Up to now, much work has been done to develop methods and theories for the design problem of optimal stiffener layout of plate/shell structures in aerospace industry and

improve structural mechanical and frequency obviously.

Besides optimization technology is also applied to optimize other ship structures, the reason of adopting optimization technology is that, The weight of the empty ship in most ships account for more than 30% of the ship total drainage, and some ships can even reach 70%--95% (passenger ship, tugboat, fishing Boat and so on) [12]. which can be seen that the weight of ships directly affects its performance parameters. So, in the design of the ship, how to design a structural layout with light weight, high stiffness and strong strength is the most difficult problem for us to reduce the weight of the ship. the traditional ship design process is based on the designer's experience or reference to the previous ship type, and then through the test and data analysis, the final ship design results are obtained. if the designed structure cannot meet the requirements of the ship, modifying the given parameters and repeat the design several times to meet the actual requirements. the workload of this method is large and cumbersome. At the same time, the design process relies too much on the experience and judgment of designers, and lacks the criteria and basis for design. the optimization technology method can solve the above problems well by setting and analyzing the design requirements, it establishes the mathematical analysis model based on the basic mechanics principle and the common finite element theory with the help of the large optimization software such as CAD and CAE, and then chooses some suitable algorithms to solve it. complete the preliminary design of topology layout, material ratio and so on. structural topology optimization can greatly improve the performance of the ship structure or reduce the weight of the ship structure under the condition of keeping the original stiffness unchanged, a better optimization results are obtained. it can bring the direct economic benefit from the energy saving and environmental

protection angle, and realize the green manufacturing. many ship designs exzamples have been applied based on optimization technology. Such as, according to the theory of genetic algorithm, he optimized the structure of the bulkhead of the submarine. at the same time, the neural network learning method was applied to the calculation process. after optimization, the bulkhead structure of the submarine has been reduced by 18.3% compared with original bulkhead weight[13]. Z.Sekulski adopted the genetic algorithm to optimize the design of a catamaran, the objective function is the weight and surface area of the hull, and the fitness function is weighted to choose the genetic calculation. And the final result shows that this algorithm is very effective for the multi-objective optimization technology[14]. Ehlers used particle swarm optimization algorithm to optimize the application of high strength steel in ship structure, this algorithm is aimed at optimizing the analysis of the utilization rate of high strength steel hull when the ship is in collision. The biggest advantage of the algorithm is that it can solve the problem of collision nonlinear computation very well[15]. Zhang used multistage optimization technology to optimize the trimaran, promting ship materials can be fully utilized based on meeting the requirements of stiffness and strength[16]. Chang use shape and size optimization method to optimize the water canon base on a fire ship, its mechanical property are improved obviously[17]; Zhang use a combination optimization method to change ship crane boom section, and its weight decrease by15.3%[18] and so on.

In view of the practicability of the optimization technology, in this paper we adopt two-stage optimization (topology and size optimization) to arrange stiffener layout and adjust its size in ship prow (SP). Besides Integration shape and size optimization is used to optimize radar mast.

1.2 Two-stage optimization method

This section explains the general mathematical concepts used for the formulation of the two-stage optimization problem in this work. We explore an optimal material layout points where the reference domain is divided into void and solid elements.

1.2.1 Topology optimization

Topology optimization is one kind of structural optimization method, the structure optimization includes topology, shape and size optimization, which are shown as figure 1.1.
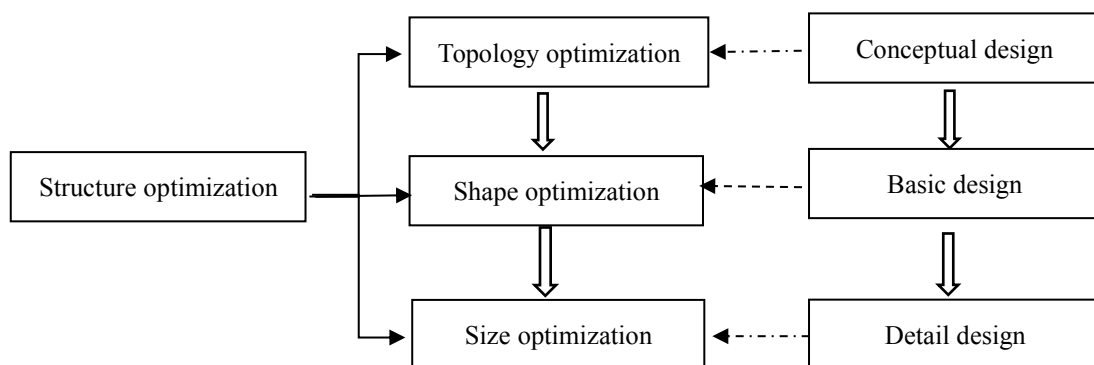
Figure 1. 1 Three levels of structural optimization method

The main difference between topology optimization method (TOM) and traditional optimization method is the method used to generate the initial shape. the TOM design process is shown in the figure 1.2

TOM is a mathematical method that optimizes material layout within a designated design area. the initial region generated by this method is closer to the final design scheme, therefore, in can reduce the iteration steps and save computing time. besides this method has more design freedoms and can get more design space compared with shape and size optimization. The following figure 1.3 visualizes the differences in

these three kinds of optimization method.
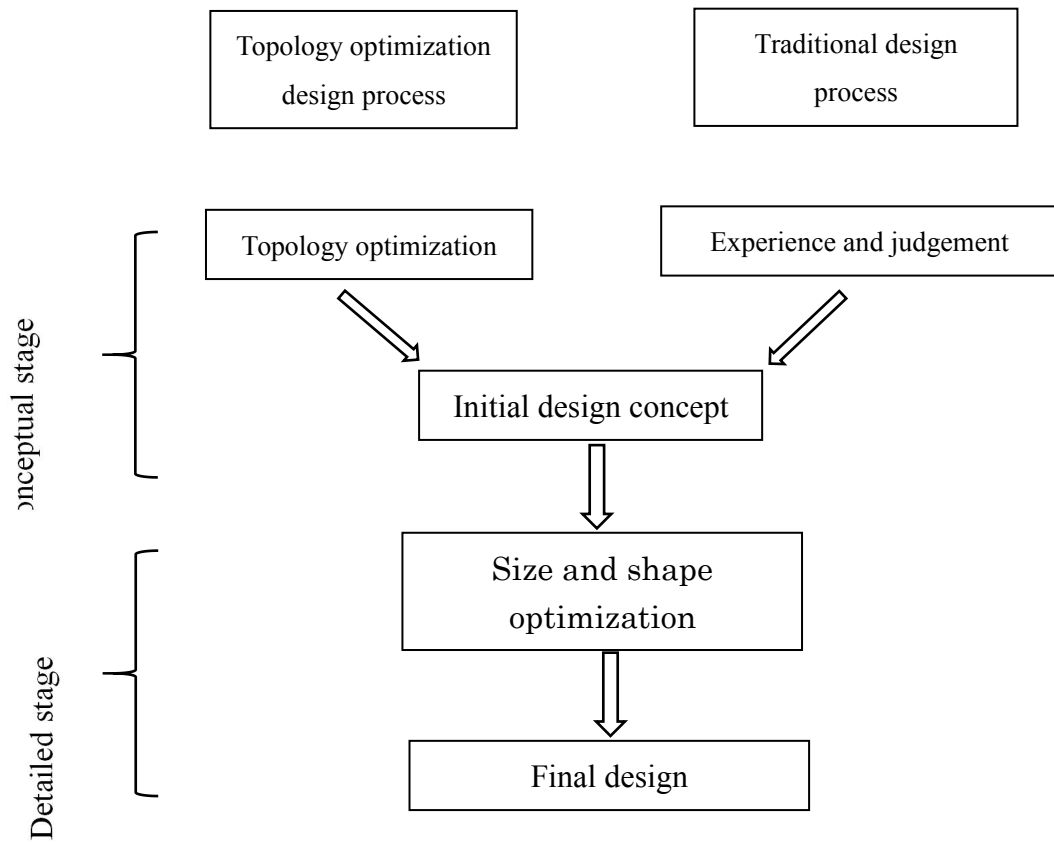
Figure 1. 2 Topology optimization role in the design process

Topology optimization

Shape optimization
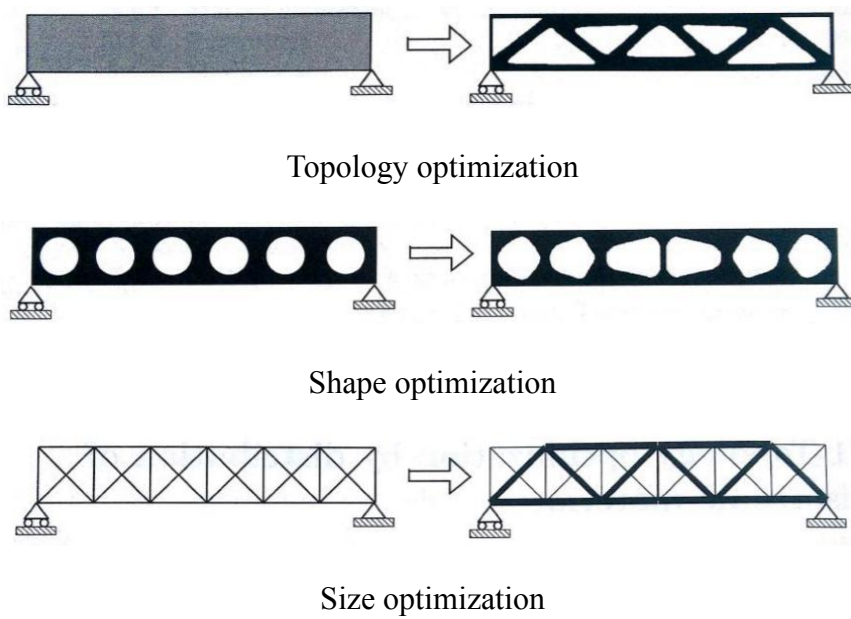
Size optimization

Figure 1. 3 Types of structural optimization[19]

The essence of topology optimization based on material interpolation model is to find the optimal material layout within the given design area, in other words, to determine which areas are void area (without material) and which areas have materials within the given design space. The mathematical model is as follow equation,

$$E_{ijkl}(\rho) = \rho E_{ijkl}^0$$

$$\rho_e = \begin{cases} 1 & \text{If } e \in \Omega_{mat} \\ \\ 0 & \text{If } e \in \Omega \backslash \Omega_{mat} \end{cases} \tag{1.1}$$

And a volume constraint

$$\int_{\Omega} \rho d\Omega = \text{Vol}(\Omega_{mat}) \leq V$$

Here, E_{ijkl}^0 is the material elasticity modulus; Ω is the given design domain; Ω_{mat} is the optimal area with material; ρ is variable density; ρ_e is element variable density; V is the volume of the initial design domain. When $\rho_e = 1$ indicates this element is an entity unit, $\rho_e = 0$ indicates this element is void.

Obviously, this is a typical 0-1 discrete variable optimization problem. When the model is complex, due to lacking an effective large-scale discrete variable optimization algorithm, the exact solution of the problem usually cannot be obtained. therefore, we use continuous variables instead of discrete variables to deal with this problem, and adopt the Solid Isotropic Material with Penalization (SIMP) algorithm to deal with the intermediate density between 0 and 1 which are generated by the continuous variables[19].

This paper mainly introduces the topology optimization method based on Solid Isotropic Material with Penalization (SIMP) algorithm. the SIMP method is derived

from the homogenization method, but the process is simple[20]. this algorithm punishes the intermediate density by introducing the penalty factor, which promote the value of intermediate density to 0/1 end, it is beneficial to obtain a better discrete structure. In this case, the intermediate density unit corresponds to a very small modulus of elasticity, so the effect on the stiffness matrix will be smaller.

The new mathematical model based on Solid Isotropic Material with Penalization (SIMP) algorithm are shown in the follow equation,

$$\mathrm{E}_{ijkl}(\rho) = \rho^p E^0_{ijkl}$$

$$0 \le \rho_{min} \le \rho \le 1 \qquad\qquad (1.2)$$

$$\int_\Omega \rho d\Omega = \mathrm{Vol}(\Omega_{mat}) \le \mathrm{V}$$

where, p is the penalty factor ($p > 1$); ρ_{min} is the lower density value limit to avoid singularities.

The density intermediate interpolation is carried out between the material characteristic values,

$$E_{ijkl}(\rho = 0) = 0, E_{ijkl}(\rho = 1) = E^0_{ijkl} \qquad (1.3)$$

The selection of the penalty factor p is related to the Poisson ratio of the material, which will be talked in the following content.

Restricting to 2D plane elasticity, assume that SIMP model is composed of two materials. One's density is 0(void) and another density is ρ.Then the bulk modulus k and shear modulus μ in elasticity tensor E of this artificial material should satisfy the so-called Hashin-Shtrikman bounds

$$0 \le \mathrm{k} \le \frac{\rho k^0 \mu^0}{(1 - \rho)k^0 + \mu^0}$$

$$(1.4)$$

$$0 \leq \mu \leq \frac{\rho k^0 \mu^0}{(1-\rho)(k^0 + 2\mu^0) + k^0}$$

Where, k^0 and m μ^0 represents the bulk modulus and shear modulus of material with density ρ.

And the Young's modulus should satisfy

$$0 \leq E \leq E^* \leq \frac{\rho E^0}{3 - 2\rho}, \qquad 0 \leq \rho \leq 1 \qquad (1.5)$$

Isotropic materials have the relationship

$$k^0 = \frac{E^0}{2(1-\upsilon)}, \mu^0 = \frac{E^0}{2(1+\upsilon)} \qquad (1.6)$$

Substituting formula 1.6 into formula 1.4, we have

$$0 \leq \frac{\rho^p E^0}{2(1-\upsilon)} \leq \frac{\rho E^0}{4 - 2(1+\upsilon)\rho}$$

$$0 \leq \frac{\rho^p E^0}{2(1+\upsilon)} \leq \frac{\rho E^0}{2(1-\rho)(3-\upsilon) + 2(1+\upsilon)} \qquad (1.7)$$

From formula 1.7, the penalization power p should satisfy

$$\text{p} \geq p^*(\upsilon) = max\left\{\frac{2}{1-\upsilon}, \frac{4}{1+\upsilon}\right\} \qquad （1.8）$$

When poisson's ratioυequal to 1/3, The minimum value of the penalty factor is 3.

For a three-dimensional problem, the penalty factor *p* can be obtained from a similar process to satisfy the follow equation.

$$\text{p} \geq max\left\{15\frac{1-v}{7-5v}, \frac{3}{2}\frac{1-v}{1-2v}\right\} \qquad （1.9）$$

When poisson's ratioυequal to 2, The minimum value of the penalty factor is 3.

both for 2D and 3D problems a penalization power p > 3 in (1.8) and (1.9) ensures that the Hashin-Shtrikman bounds can be satisfied, so that the SIMP model can be realized as its stiffness varying with ρ and FEM singularity problem is avoided. Thus, the SIMP model yield relatively nice results and this simplicity of the penalization power p facilitates the implementation of topology design in commercial finite element codes.

The mathematical model based on SIMP is shown as follows,

$$\min(\rho) \quad C = F^T U$$

s.t: $\quad V = f \cdot V_0 \leq V$

$$F = KU \qquad\qquad (1.10)$$

$$0 < \rho_{min} \leq \rho \leq 1$$

Here, C is structure compliance, U is displacement matrix, K is stiffness matrix, f is volume ratio.

For discrete structures, $V = f \cdot V_0 = \sum_{e=1}^{N} x_e v_e$, the structure compliance equation can be modified as follow,

$$C = F^T U = U^T K U = \sum_{e=1}^{N} u_e^T k_e u_e = \sum_{e=1}^{N} (x_e)^p u_e^T k_e u_e \qquad (1.11)$$

The sensitivity based on equation 1.11 are shown in the follow equation,

$$\frac{\partial C}{\partial x_e} = - U^T \frac{\partial K}{\partial x_e} U = - \sum_{e=1}^{N} u_e^T \frac{\partial k_e}{\partial x_e} u_e = - p(x_e)^{p-1} \sum_{e=1}^{N} u_e^T u_e k_e \qquad (1.12)$$

The sensitivity equation of volume constraint can be written as follow,

$$\frac{\partial V}{\partial x_e} = \sum_{e=1}^{N} \frac{\partial(x_e v_e)}{\partial x_e} = \sum_{e=1}^{N} v_e = V_e \qquad (1.13)$$

Where, x_e is relative density; u_e is the column vector of element displacement; k_e is the element stiffness matrix after optimization; v_e is element volume after optimization.

Classical topology optimization formulation

The typical topology optimization problem formulations based on equation (1.9) are given in the form 1.1.

Type	Objective	Constraint
A	Minimize compliance (Strain energy)	Volume/Volume fraction (or Mass)
B	Minimize volume/mass	Maximum Displacement
C	Minimize volume/mass	Maximum Global Stress
D	Minimize volume/mass	Minimum Buckling factor (1.0)

Table 1. 1 Typical optimization formulation

The type A about minimizing the structure compliance is the most common topology optimization type. that is to say, to maximize the structure stiffness based on volume fraction within given design area. The best volume fraction is about 0.3, which have been prove that this fraction can promote topology optimization to get a clearer results[21]. Type B and type C are also often applied to optimize the actual engineering problem[22, 23]; about thin plate structure, buckling is the most important constraint for thin structure, type D is often used[24, 25].

optimization algorithm

The solution process for topology optimization is a large scale, because every iteration need to call for structural analysis, which leading to solution process become difficulty. The overall structural response is obtained by solving structural finite element response, and the structural response function is a stealth nonlinear function about the design variable. based this, the optimization objective and constraint are calculated by

adopting appropriate algorithm, then the optimal solution can be found after many iterations. So, the main current algorithms for topology optimization are optimality criteria method (OCM)[26] and mathematical programming schemes (MP)[27] based on the above-mentioned characteristics.

MP algorithm includes sequential linear programming and sequential quadratic programming and so on. This method is suitable different types of optimization problems. The results have high reliability and better accuracy, but this method requires repeated computation of objective function and constraint function value and sensitivity, resulting in long solution time. So, this method is good at solving multi-constraint, topological optimization problems with different objectives[28, 29].

In this paper, sequential quadratic programming method is applied to solve the topology optimization problem, the detailed optimization process is shown in the figure 1.4.

OCM include optimality criteria, continuum-based optimality criteria, discretized criteria and discretized continuum optimality criteria. The solution procedure of the optimization criterion is independent of the number of design variables, So the process of solving is simple and its convergence is faster, the optimization criterion method is usually applied to solve single objective functions or single constrained optimization problems[30, 31].

```
                          ┌──────────┐
                          │  Start   │
                          └────┬─────┘
                               │
                               ▼
                  ┌────────────────────────────┐
                  │ Define design area, boundary │
                  │        constraints           │
                  └──────────────┬──────────────┘
                                 │
                                 ▼
                  ┌────────────────────────────┐
                  │     Generating element       │
                  └──────────────┬──────────────┘
                                 │
                                 ▼
                  ┌────────────────────────────┐
                  │   Initialization of design   │
                  │         variables            │
                  └──────────────┬──────────────┘
                                 │
                                 ▼
                  ┌────────────────────────────┐
         ┌───────►│  construction of the element │
         │        │      stiffness matrix        │
         │        └──────────────┬──────────────┘
         │                       │
         │                       ▼
         │        ┌────────────────────────────┐
         │        │    finite element analysis   │
         │        └──────────────┬──────────────┘
         │                       │
         │                       ▼
         │        ┌────────────────────────────┐
         │        │    Objective function and    │
         │        │        sensitivity           │
         │        └──────────────┬──────────────┘
         │                       │
         │   ┌────────────────────────────┐
         │   └──►│ Iteration of design variables │
         │        └──────────────┬──────────────┘
         │              No        │
         │        ◄───────┤       ▼
         │        ┌────────────────────────────┐
         │        │      Volume constraint       │
         │        └──────────────┬──────────────┘
         │                       │
         │  No                   ▼
         └───────┤  ┌────────────────────────────┐
                    │        convergence           │
                    └──────────────┬──────────────┘
                                   │
                                   ▼
                    ┌────────────────────────────┐
                    │          results             │
                    └──────────────────────────────┘
```
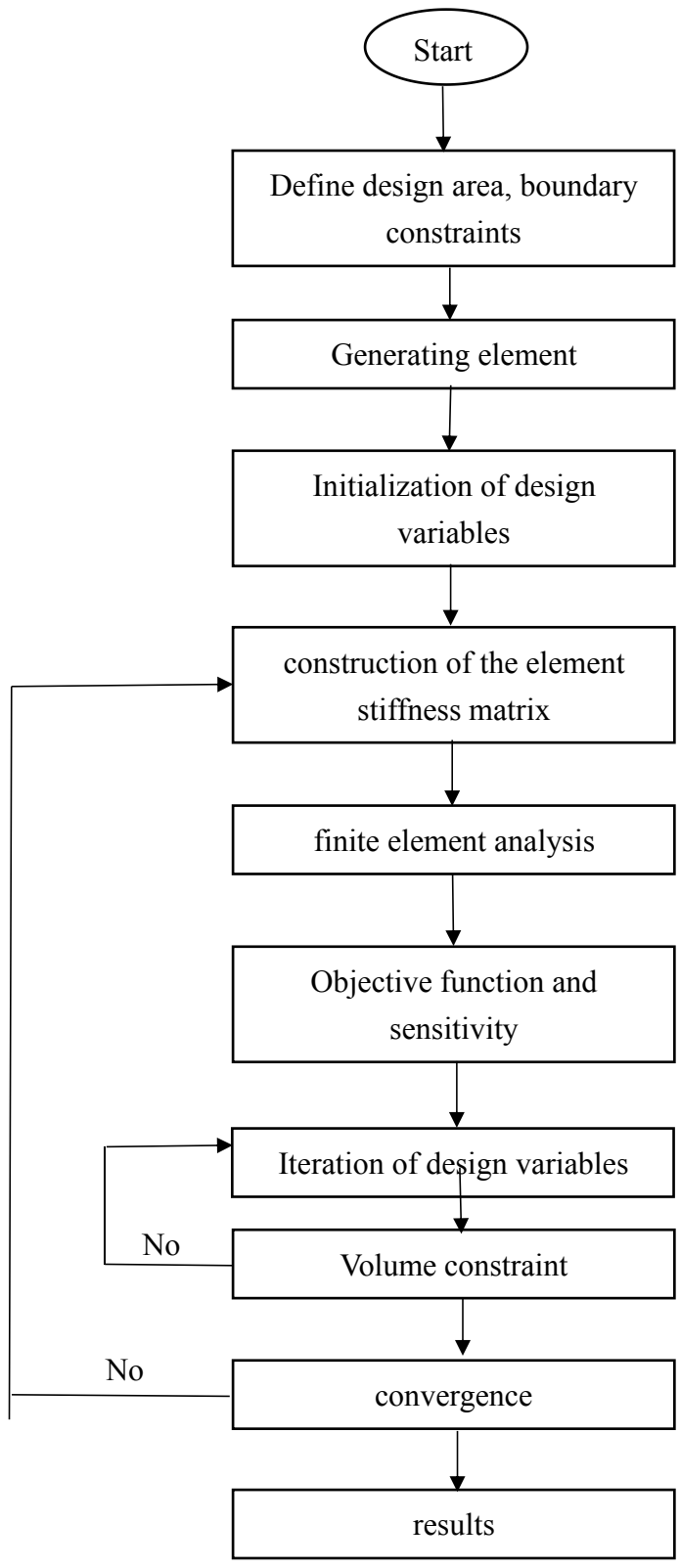
Figure 1. 4 Topology optimization process

13

Numerical instability phenomenon

Chequerboard patterns

Checkerboard refers to the periodic variation of design variables between 0-1 densities in a structural optimization results area, that is, periodic changes in the distribution of entities and holes[32, 33]. The appearance of checkerboard pattern is the result of density penalty which makes elements too rigid.

Checkboard

Ideal results

Figure 1. 5 Checkerboard pattern[19]

Mesh dependency

Mesh dependency means the topology optimization results is relate to the element numbers, different element numbers will produce the different optimization results[33, 34], as figure 1.6 shown. when the element numbers are excessive, there will be many rod-shaped structure to be generated, which decrease the manufacturability for optimization results.
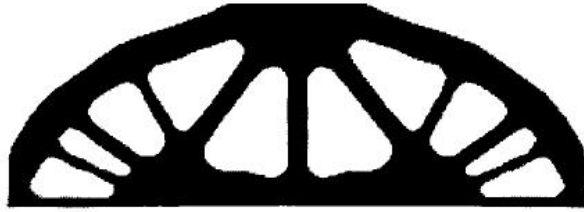
Element number (100×240)
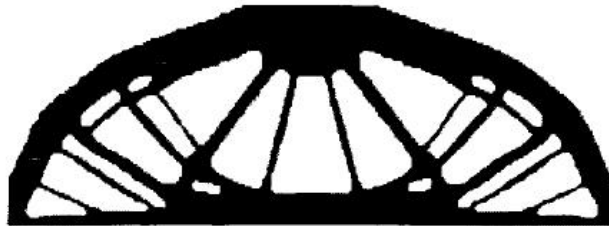
Element number (120×288)

Element number (140×336)

Figure 1. 6 Mesh-dependency problem[35]

The two phenomena of checkerboard and grid dependence generally appear in the result of topology optimization at the same time. the method that can effectively remove the checkerboard can also effectively overcome the grid dependence. The commonly used methods are mainly the following,

High order element method.

Diaz and Sigmund's research shows that selecting high order elements reasonably can effectively reduce or eliminate the above phenomena[32]. the disadvantage of this method is that the computation is too large, so it is not very practical.

Perimeter constraint method.

Haber proposed a method that suppressing the formation of checkboard by restricting the perimeter of optimization results[36]. they think that for the same empty area, the more the number of holes, the greater the total circumference of all holes, When the number of holes allowed by design increases gradually, the checkerboard phenomenon appears in optimization. But the upper limit of the circumference constraints requires experience to determine. that is to say, the circumference of the constraints, its value must be properly adjusted to achieve the optimal value, and its optimization result may be a local optimal.

Local gradient method

Petersson adopted the to limit the change of the density of the adjacency element [37], This method can prevent the generation of partial fine lines, thereby reducing the geometric complexity of the mechanism topology, but the optimization results are difficult to satisfy the global optimum, Moreover, this method produces many additional constraints in the optimization problem, which greatly reduces the computational efficiency.

element filtering method[30]

this method is used in this paper to suppress the checkboard and mesh dependency phenomenon. The modified mathematical model can be formulated as follows:

$$\rho_i \geq \max \left[\mu, \rho_j - (1.0 - \rho_{min})dist(i,j)/r_{min}\right] \qquad (1.14)$$

where subscripts i and j denote the element location in the coordinate system, μ is the lower limit of relative density, ρ_j is the highest density of element j at the previous

iteration among all elements that are adjacent to element i, dist(i,j) denotes the distance between the centers of elements i and j, and r_min is half the predetermined minimum member diameter. Additionally, using a quadratic mesh in the optimization process can avoid the checkerboard problem to some extent.

1.2.2 Size optimization

Size optimization (parameter optimization) is applied in the detailed design stage based on the determined structural style; an overview of size optimization is summarized by Kirsch [38]. it mainly modifies and optimizes the size of the model (structural-element parameters), so the shape of the model structure will not be changed. the object of size optimization includes the following[39]: a, beam cross section area. b, The length or diameter of a rod. c, plate thickness. d, the layer thickness and angle of composite material. e, spring stiffness. Size optimization is performed analytically. A nonlinear objective function or constraint is transformed into a linear expression by a linear approximation method. However, the structural topological relationship and element shape remain unchanged during the solution procedure, which is why size optimization merely changes the structural-element properties.

As figure 1.6 shown, the sectional area of the truss is optimized by size optimization.
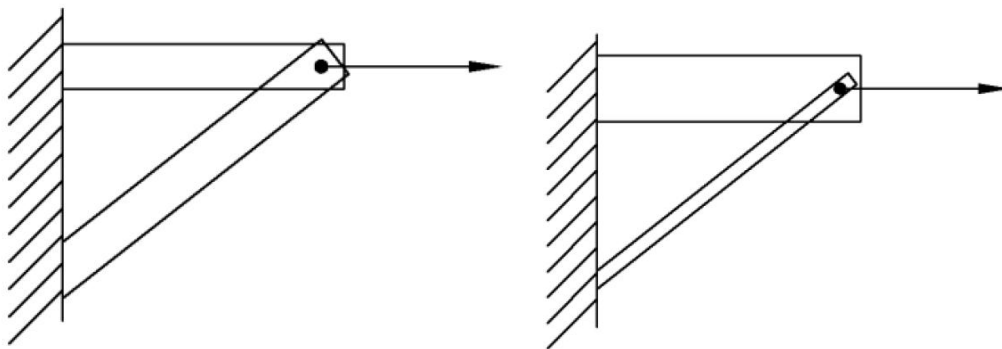

Figure 1. 7 Truss size optimization

Taking the above optimization objects as design variables, the objective function can be optimized under the premise of considering the constraints. And the constraint conditions of size optimization include the following: a, element stress constraint. b, strain energy constraint. c, node displacement constraint. d, modal constraint and so on. Some structural elements have multiple parameters depending on each other; like beams in which the area, moments of inertia, and torsional constants lie on the geometry of the cross section.

The structural-element property is not design variable for size optimization, but the property can be defined as design variables function, the equation is as follow,

$$\gamma = C_0 + \sum DV_i \cdot C_i \qquad (1.15)$$

where γ is the property to be optimized, C_0 is a constant, and C_i are linear factors associated to the design variable DV_i.

If there are multiple design variables, a correlation functions can be established among these variables, the equation is written by the linear combination expression,

$$DDVID = C_0 + CMULT \sum C_i \cdot IDV_i \qquad (1.16)$$

Where CMULT is Constant multiplier, IDV_i represent identification number of independent design Variable, C_i coefficient multiplier for IDV_i.

At present, the most commonly used algorithm for solving size optimization is method of feasible direction, which is one kind of mathematical programming method[40]. the essence of the feasible direction method is to obtain the optimal design point in the favorable direction based on the location of the design points in the n-dimensional design space. one of the notable features of this method is that it can deal with optimization problems with various properties of constraints at the same time, that is, it

has better adaptability for different optimizations problems. The detailed solution process will be talked in the chapter3.

Besides free size optimization is also often applied in practical product design, especially in the design of Aeronautical parts[41]. The design variable is element thickness for free size optimization, this optimization method allows the shell thickness change from T to T_0 freely, which is different from topology optimization obviously. The detailed differences in the characteristics of topology and free-size are summarized in the following table. Generally, in topology optimization, the thickness of solid elements is optimized well, but it is not accurate when executing on shell elements. Thickness is set as design variable in free size optimization, which provides a direct repair for the accuracy problem of the shell elements.

Figure 1. 8 Shell cross-section

	Shell topology optimization	Free-size optimization
Goal	0/1 thickness	Variable thickness（$\geq T_0$）
Results	Truss-like design concepts	Variable thickness panel likely for in-plane loading

Table 1. 2 Characteristics of shell topology vs free-size

1.2.3 Layout-size optimization

In recent years, some researchers propose a two-stage optimization method combining topology and size optimization as a synthetic tool for the conceptual and detail stiffener design of structure. Two-stage method not only optimize stiffener location by

above-mentioned topology optimization techniques, but also optimize stiffener dimension further by size optimization. Analysis based on topology and size optimization method are typically applied to numerous application case, these case results demonstrated two-stage method were feasibility. Locatelli and Mulani et.al adopted two-stage optimization method to optimize the supersonic wing leading edge ribs, rib configurations are determined based on topology results, later size optimization is adopted to optimize skin and rib thickness simultaneously, and reduce the total weight by 18.4%[42]; Teknisk Mekanik adopts this method to optimize vehicle body structure, based on two-stage optimization, achieving a high stiffness of the front structure for improving ride and handling[43]. Meanwhile there are also some successful example in shipbuilding industry. Two-stage optimization is used to optimize stiffener layout and size for a complex composite ship structure based on limit wave load conditions, the results show a weight saving of up to 19% over the original model[44]. Qiu et.al applied two-stage optimization method to generate stiffener for tanker structures in cargo tank region, and got a good performance[45]. Two-stage optimization were also used in three-dimension stiffener layout, getting a better stiffener location layout. M. Grujicic used this method in an ongoing research project aimed at the development of short lead-time lightweight automotive BIW structural components with efficient stiffness, strength and buckling performance[46]. Fan adopted this method to optimize the stiffener layout and size on panels of spaceborne and got a satisfactory structure[47]. Chen adopts this method to optimize the reinforced ribs for a machining center, its eigen frequency become larger beyond given frequency compared with original model, a reasonable optimization result is obtaine[48].

In order to make stiffener layout result more clear and accurate through 3D topology optimization, some manufacturing technologies are considered during optimization process such as multi-directional, casting, extrusion and so on. Leiva and Waston et.al optimized stiffener layout and size by multi-directional constraint, get a reasonable structure[49].Zhu and Gu et.al proposed casting constraints based on Heaviside function to optimize engine structure and get a lightweight engine[50]. Other better stiffener layout optimization result based on manufacturing constraints, we can see from[51]. The optimization results of topology optimization based on manufacturing constraint prove that this method is an effective and actual strategy for stiffener layout design.

1.3 Integration shape and size optimization

Size optimization method has been talked in the above section, so in the follow section we will talk about shape optimization which be used in the integration optimization method. The shape process is shown in the following figure 1.9,

1.3.1 Shape optimization

Shape optimization is to find the best geometric shape within the boundary conditions, by changing the nodes displacement, and then get better performance (minimize the structure material, reduce the stress concentration, improve rigidity and so on)[52].

In finite element method, the structure geometric shape is modified by the vector of node coordinates. for fear of avoiding the deformation of the mesh caused by the shape change, the change of the shape of the boundary for the structure should be transformed into the internal change of the mesh[53].
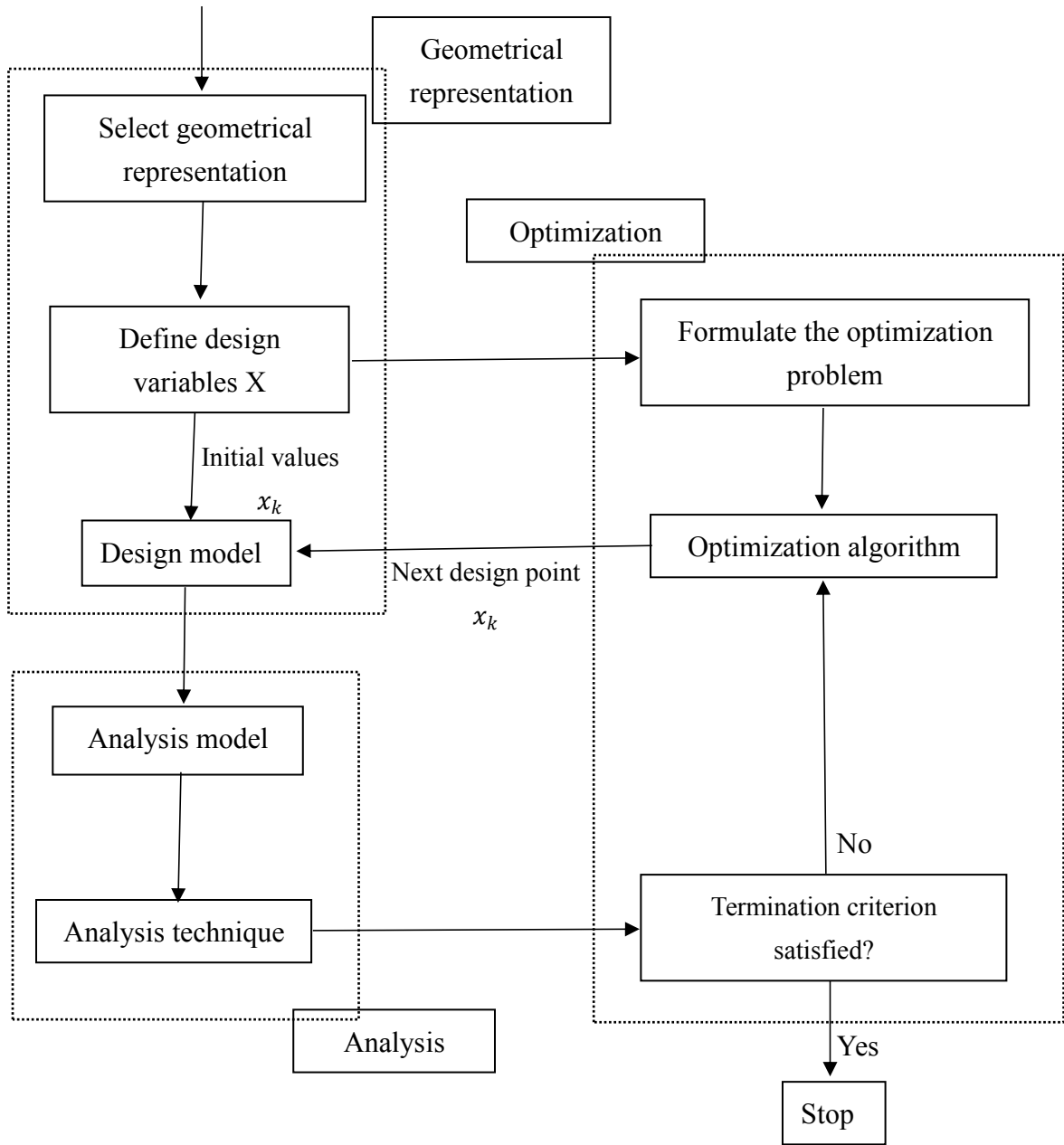
Start

Figure 1. 9 The process of shape optimization

The principle is applied to expound mesh changes in the process of shape optimization

is the perturbation vector approach[54], the mathematical equation (1.17) as follow,

$$X = X_0 + \sum DV_i \cdot PV_i \qquad (1.17)$$

Where, X is node coordinate vector, X_0 is the initial coordinate vector of the node,

DV_i is design variable, PV_i is the perturbation vector associated to the design variable.

The problem of shape optimization mainly includes the following difficulties compared with other optimization methods,

(1) Shape control problem

The problem is to change the node's coordinates in the space without changing the number of elements and nodes in the original structure to obtain the better structure shape. when changing the location of the nodes, the element shape may be distorted, which lead to subsequent optimization cannot be carried out normally. therefore, mesh adaptation technology is needed to ensure mesh quality and iterative accuracy.

(2) Shape sensitivity analysis

Sensitivity analysis directly affects the numerical accuracy and computational efficiency of structural state response to design shape design variables. And the computation of sensitivity analysis accounts for about half of the total optimization process. So, it is very important to improve the computational efficiency and accuracy of shape sensitivity.

In recent years, shape optimization has been widely applied in the structural design of products. Zhou adopt shape optimization method to change the shape of E-model electrodynamic shaker bracket, the frequency range of shaker is broadened and its weight is reduced obviously[55]; Liu use this method to optimize the motorcycle seat cushion bottom plate, its first-order frequency and stiffness improve greatly, and its mass reduce by 19%[56]. Yang optimize the shape of rocket launcher canister based on shape optimization, its mass reduces 12.7%, the deformation and stress which the

canister subject are in a reasonable range[57]. Yang take the main beam of crane as object, adopt shape optimization based on hyperworks software to improve its stability and get a better result compared with original structure[58]; Fang add the mesh deformation to shape optimization, and propose the multi-objective shape optimization based on surrogate model, Apply this method in vehicle body, the stability of vehicle body improve greatly[59]. There are also lots of engineering examples about shape optimization, please refer to related papers[60-62].

1.3.2 Integration optimization method

The integration optimization method is the combination shape optimization and size optimization[63], during optimization process size optimization is adopted to achieve design requirements by changing the properties of the structural unit. shape optimization is to change the structure shape parameters, such as beam section area, shell element thickness, so that the optimized structure meets mechanical properties requirements.

The key issue of this optimization method is to coordinate the relationship among design variable, objective function and the criteria of the optimal solution convergence. This issue can be expressed by the following equation (1.18), if the value of $\lambda_1, \lambda_2, p, q$ are determined, the optimal solution will be obtained.

$$f(X^{n+1}, A^{n+1}) = f(X^n + \lambda_1 p, A^n + \lambda_2 q) \qquad (1.18)$$

A is the radar mast thickness, X is the shape change, λ_1, λ_2 are iteration step, $p = A^{n+1} - A^n$ 、 $q = X^{n+1} - X^n$ are the iteration vector direction of the size and shape design variables.

1) Design variable

Size optimization is applied to optimize the structure thickness, so the design variable is radar mast thickness A; shape optimization is used to optimize the structure shape (node displacement), so the design variable is shape change X. the design variables of radar mast are defined as follow,

$$A = \{A_1, A_2, A_3, \cdots A_n\}^T$$
$$X = \{X_1, X_2, X_3, \cdots X_m\}^T \tag{1.19}$$

2) Constraint function

The boundary condition function should meet the following requirements in this chapter,

$$\sigma_i \leq [\sigma]$$
$$\omega_i \geq [\omega]$$
$$A_i^L \leq A_i \leq A_i^U \tag{1.20}$$
$$X_i^L \leq X_i \leq X_i^U$$

Here, $[\sigma]$ is allowable stress, $[f]$ is allowable frequency, X_i^L and X_i^U are the range of shape variable; A_i^L and A_i^U are the range of radar thickness.

3) Objective function

The goal of this chapter is to realize the lightweight design for radar mast, so the objective function is to minimize volume

$$\text{Min } V(X) = \sum_{i=1}^{n} S_i \cdot L_i \tag{1.21}$$

The detailed process of finding the optimal solution within the integration optimization are shown in the figure 1.10 and figure 1.11.
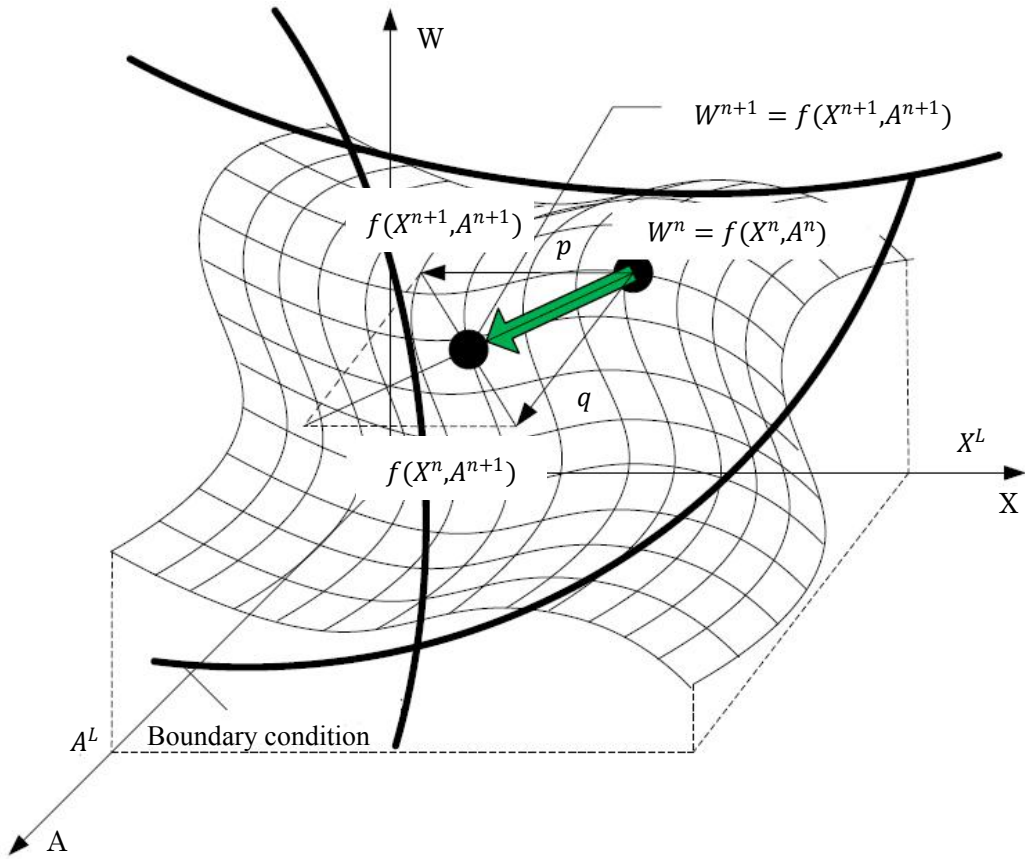
Figure 1. 10 Iteration graph of design points in feasible design domain

this chapter uses the experience median method to update the design variables, which can reduce the possibility that the next iteration point is not in the feasible area[64]. The criterion of optimal solution is the absolute value of objective function difference after size optimization and shape optimization. when the absolute value is smaller than a specified value ε (in this chapter, the specified value that we adopt is 0.03), it is considered that the optimal solution of the radar mast structure has been found, which shows that the objective function is not further reduced after size and shape optimization[65].

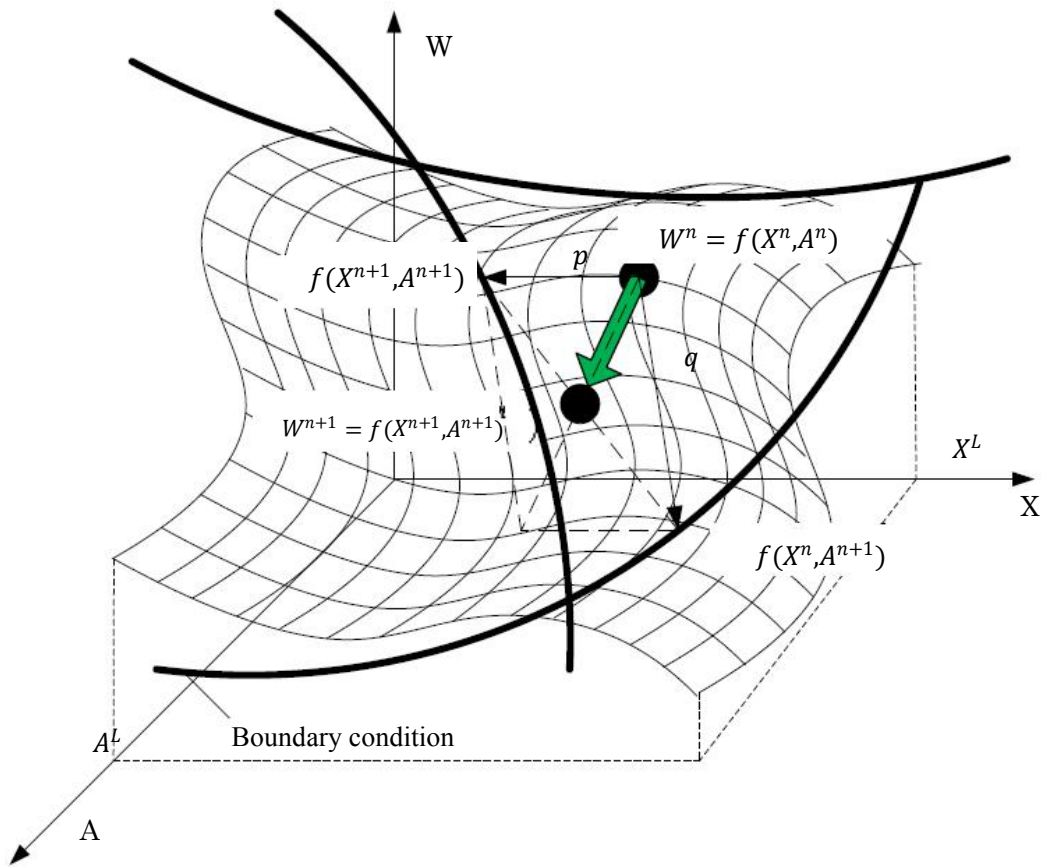Figure 1. 11 Iteration graph of design points on the boundary of the feasible domain

From the figure we can know that, W^n, A^n , X^n are respectively the objective function, shape design variable and size design variable of the n-th iteration step. The absolute value of the difference of integration optimization is norm of $p - q$ vetor. When the length of the gradient is small enough, we can think that the objective function value is very close to the last point, we can infer that the optimization problem has got the best solution. In order to simplify the problem and explain the principle, figure 1.10 and figure 1.11 simplify the dimension design variables and the shape design variables into one-dimensional design variables.

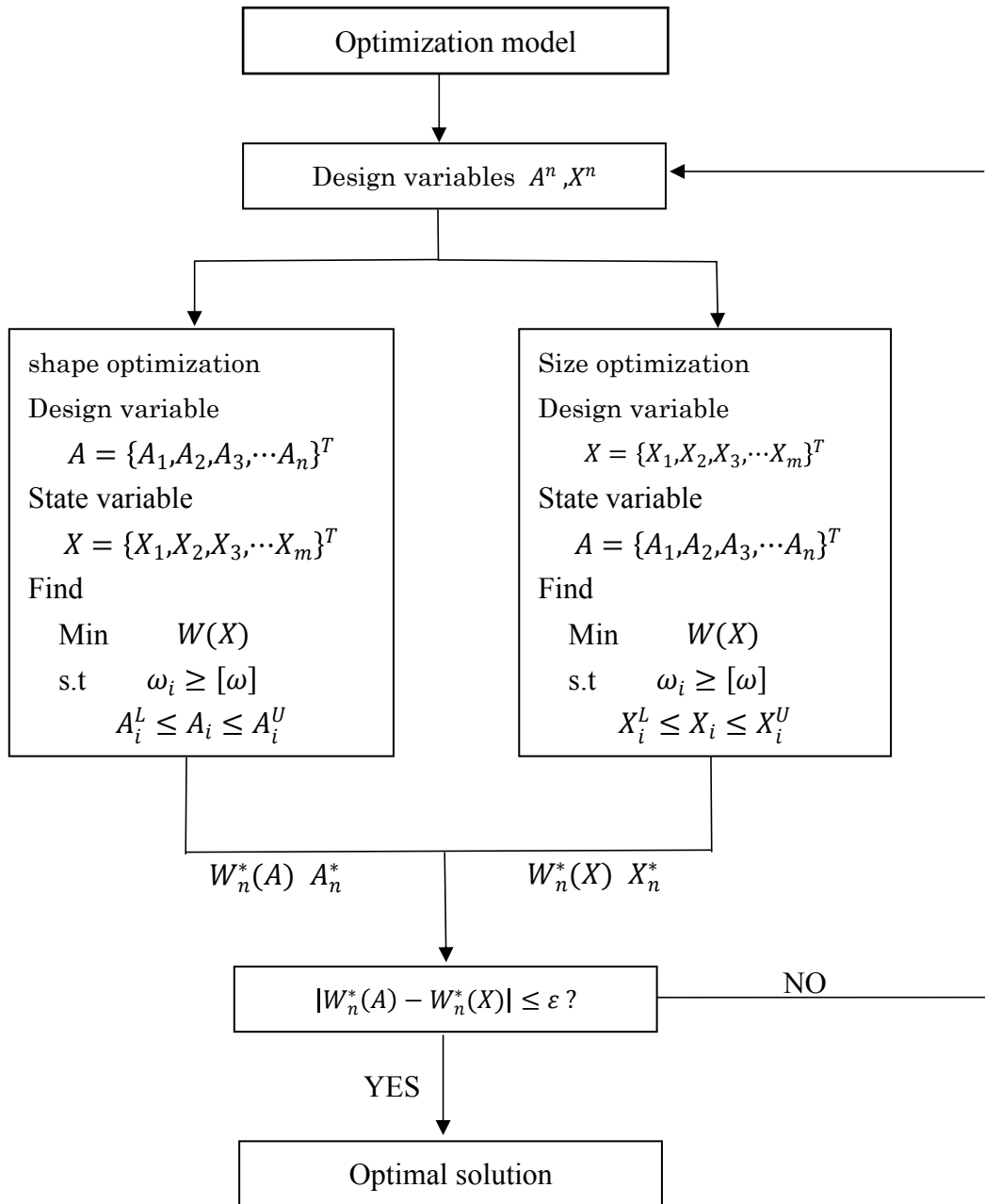The detail integration optimization process can be shown in the following figure,

Figure 1.12 Integration optimization process

The integration optimization method is considered as a powerful tool of improving the traditional structural designs in many practical applications.

Wu adopted size and shape optimization method to optimize web plate height and thickness of crane, the minimum structure weight is achieved on the premise of

satisfying its stiffness and strength[66]; Ye applied size and shape optimization to optimize the wing rib of A380 while manufacturing processes, buckling requirements are took into account, the result shows that about 44% of its weight has been reduced[67]. Zhang also adopted this method to optimize aircraft tail whose material are composite[68]. The above applications prove that integration shape and size optimization method has its rationality and practicability.

1.4 Dissertation layout and objectives

This thesis adopted two-stage method optimization method to optimize the coarse layout and size of the stiffener in ship prow，then surrogate model optimization method is adopted to determine the detail stiffener location based on the above results.

The reminder of this dissertation is organized as follow:

◆ Chapter 1

This chapter contains a brief review of the two-stage and surrogate model optimization method, introduce the optimization process and to provide the relevant background.

◆ Chapter 2

This chapter introduces the current development of stiffener layout optimization method, then construct the optimization mathematical model based on two-stage optimization method and actual load cases, and predict stiffener layout and arrange T style stiffener on account of optimization results.

◆ Chapter 3

Design variables for size optimization are selected, then size optimization model is built, getting an optimal stiffener size.

◆ Chapter 4

Integration shape and size optimization method is adopted in this chapter, considering the mutual coupling between size and shape design variable simultaneously for radar mast. And getting an effective result.

- Chapter 5

This chapter contains the conclusions based on the results observed throughout the dissertation. the radar mast is selected for the target of optimization.

Chapter 2

Stiffener layout optimization design

2.1 Ship prow structure and load cases

An LNG carrier (as figure 2.1 shown) is a tank ship designed for transporting liquefied natural gas (LNG), To facilitate transport, the natural gas is cooled down to approximately -163 °C (-261 °F) at atmospheric pressure, at which point the gas condenses to a liquid. As the LNG market grows rapidly[69], the fleet of LNG carriers continues to experience tremendous growth, the size and capacity of LNG carriers has increased greatly. As people's awareness of environmental protection has increased, reduce the manufacturing cost and enhance the competitiveness of the shipbuilding enterprises, more and more attention has been paid to light-weight design of LNG carriers.
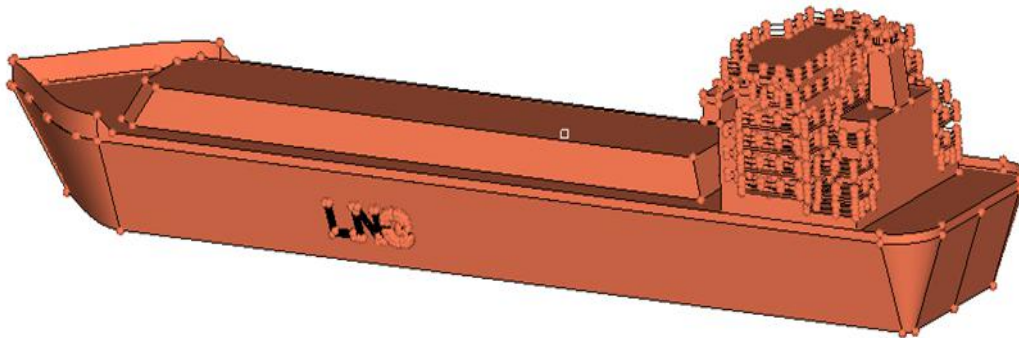
Figure 2. 1 LNG carrier

In this paper, the prow of LNG carrier is considered as research object, which is the forward-most part of a ship's bow that cuts through the water. The traditional stiffener layout in ship prow are shown in the figure 2.3, which is based on ship design manual

and engineering experience. The prow is the forward-most part of a ship's bow that cuts through the water. we consider the fore peak structure and the bottom area collectively as the research object known as the ship prow(SP). We use low-alloy Q345 steel as the structural material. The principal dimensions are as follows: longitudinal length 30,000 mm; transverse width 42,800 mm; vertical height 15,500 mm; draught depth 9,000 mm. The detail structural model is shown in Figure 2.2.
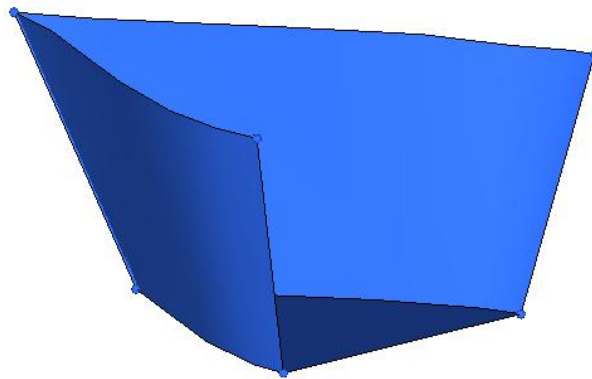
Figure 2. 2 Ship prow

No goods are stored in the SP. Rather, it is regarded as a ballast tank with which to adjust the ship's stability and floating conditions. The SP bears local external force mainly during voyage. The load conditions borne by the SP differ from those at midship.

we consider the working conditions of the ship as being the common structural rules (CSR) published by the International Association of Classification Societies. Computing the loads when the ship is fully loaded with goods, the ship reaches its maximum draught line and is therefore in its ultimate state. The load cases borne by the SP are as follows[70].
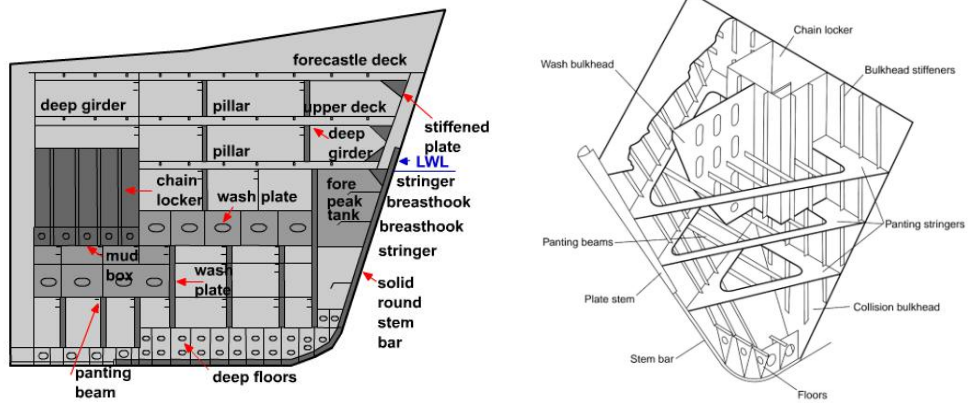
Figure 2. 3 Traditional stiffener layout

Before we calculate the load cases, the sign convention and coordinate system for ship should be determined firstly, as figure 2.4 shown,

The ship motions are determined concerning the ship center of gravity (COG),

▲Positive surge is set as the X-axis direction.

▲Positive sway is set as the Y-axis direction.

▲Positive heave is set as the Z-axis direction.

▲Positive roll motion is positive rotation along a longitudinal axis through the COG

▲Positive pitch motion is positive rotation along a transverse axis through the COG

▲Positive yaw motion is positive rotation along the vertical axis through the COG

Figure 2. 4 Definition of positive motions

Load cases

a. Dynamic load conditions

The dynamic loads connect each dynamic load case with the help of Equivalent Design Wave (EDW) thought. the EDW concept used a set of uniform dynamic loads for ships, such that specified primary load response is equal to the required long term response value.
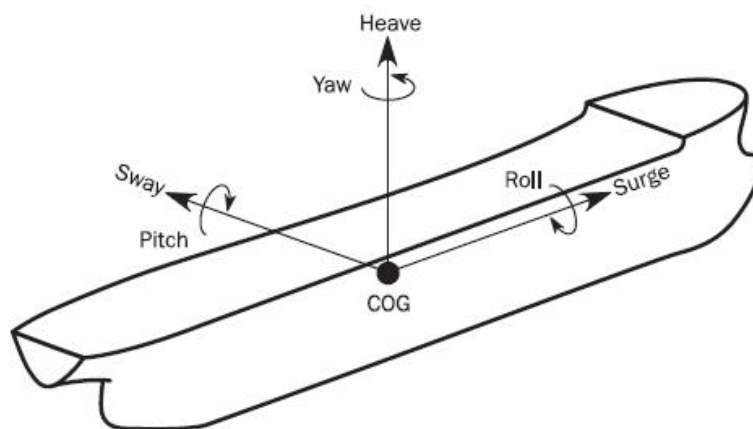
The following EDW will be applied to generate the dynamic load cases for structural evaluation:

●HSM load cases:

HSM-1 and HSM-2: Head sea EDWs are to minimize and maximize the vertical wave bending moment for ship respectively.

●HSA load cases:

HSA-1 and HSA-2: Head sea EDWs are to maximize and minimize the head sea vertical acceleration for ship respectively.

●FSM load cases:

FSM-1 and FSM-2: Following sea EDWs are to minimize and maximize the vertical wave bending moment for ship respectively.

BSR load cases:

●BSR-1P and BSR-2P: Beam sea EDWs are to minimize and maximize the rolling motion downward and upward on the port side respectively with waves from the port side.

BSR-1S and BSR-2S: Beam sea EDWs are to maximize and minimize the rollling motion downward and upward on the starboard side respectively with waves from the starboard side.

●BSP load cases:

BSP-1P and BSP-2P: Beam sea EDWs are to maximize and minimize the hydrodynamic pressure at the waterline for ship on the port side respectively.

BSP-1S and BSP-2S: Beam sea EDWs are to maximize and minimize the hydrodynamic pressure at the waterline for ship on the starboard side respectively.

●OST load cases:

OST-1P and OST-2P: Oblique sea EDWs are to minimize and maximize the torsional moment at 0.25L from the AE with waves from the port side respectively.

OST-1S and OST-2S: Oblique sea EDWs are to maximize and minimize the torsional moment at 0.25L from the aft end with waves from the starboard side respectively.

●OSA load cases:

OSA-1P and OSA-2P: Oblique sea EDWs are to maximize and minimize the pitch acceleration with waves from the port side respectively.

OSA-1S and OSA-2S: Oblique sea EDWs are to maximize and minimize the pitch acceleration with waves from the starboard side respectively.

Note 1: 1 and 2 denote the maximum or the minimum dominate load component for each EDW.

Note 2: P and S denote that the weather side is on port side and on starboard side respectively.

Actually, there are four main load cases (HSM, FSM, BSR and BSP) which need to be considered in this study, other load cases are applied to design ship structure based on the above four main load cases. So, the following table 2.1 describe the ship motions responses and the global loads corresponding to four main dynamic load cases.

Load case	HSM1	HSM2	FSM1	FSM2	BSR1	BSR2	BSP1	BSP2

EDW	HSM		FSM		BSR		BSP	
Wave type	Head sea		Following sea		Beam sea		Beam sea	
Effect	Max. bending moment		Max. bending moment		Max. roll		Max. external pressure	
VWBM	(+)	(-)	(+)	(-)	(+)	(-)	(+)	(-)

Table 2. 1 Ship response for load cases

(+) represents the sagging state; (-) represents the hogging state.

VWBM: vertical wave-induced bending moment

During optimization process, we combine the above load cases by the load combination factors. The combination factors corresponding to load cases are shown in the following table 2.2.

b.   External loads

the external pressure P_{ex} at any load point of the ship prow, in KN/m^2, about the static design load scene, which can be described as:

$$P_{ex} = P_s \qquad (2.1)$$

But greater than 0.

The total pressure P_{ex} at any load point of the hull is the static plus dynamic design load scene, which is derived from each dynamic load case and can be described as follow:

$$P_{ex} = P_s + P_w \qquad (2.2)$$

Where: P_s is hydrostatic pressure. P_w is wave pressure. These two loads are talked in the follow sections.

LCF	HSM1	HSM2	FSM1	FSM2	BSR1	BSR2	BSP1	BSP2

36

M_{WV}	C_{WV}	-1	1	-1	1	0	0	$0.4 - \frac{T_{LC}}{T}$	$\frac{T_{LC}}{T} - 0.4$
Q_{WV}	C_{QW}	-1	1	-1	1	0	0	$0.4 - \frac{T_{LC}}{T}$	$\frac{T_{LC}}{T} - 0.4$
M_{WH}	C_{WH}	0	0	0	0	$1.2 - \frac{T_{LC}}{T}$	$\frac{T_{LC}}{T} - 1.2$	0	0
a_{surge}	C_{XS}	-0.8	0.8	0	0	0	0	0	0
$a_{pitch-x}$	C_{XP}	1	-1	0	0	0	0	0	0
gsinØ	C_{XG}	1	-1	0	0	0	0	0	0
a_{sway}	C_{YS}	0	0	0	0		0	1	-1
a_{roll-y}	C_{YR}	0	0	0	0	1	-1	0.3	-0.3
gsinθ	C_{YG}	0	0	0	0	1	-1	0.3	-0.3
a_{heavy}	C_{ZH}	$0.6\frac{T_{LC}}{T}$	$-0.6\frac{T_{LC}}{T}$	0	0	$\sqrt{L}/40$	$-\sqrt{L}/40$	1	-1
a_{roll-z}	C_{ZR}	0	0	0	0	1	-1	-0.3	0.3
$a_{pitch-z}$	C_{ZP}	1	-1	0	0	0	0	0	0

Table 2. 2 Load cases combination factors

Where, the meaning of symbol in the form, please refer to [70].

Hydrostatic pressure

The hydrostatic pressure P_s at any point in ship prow, which is obtained from table
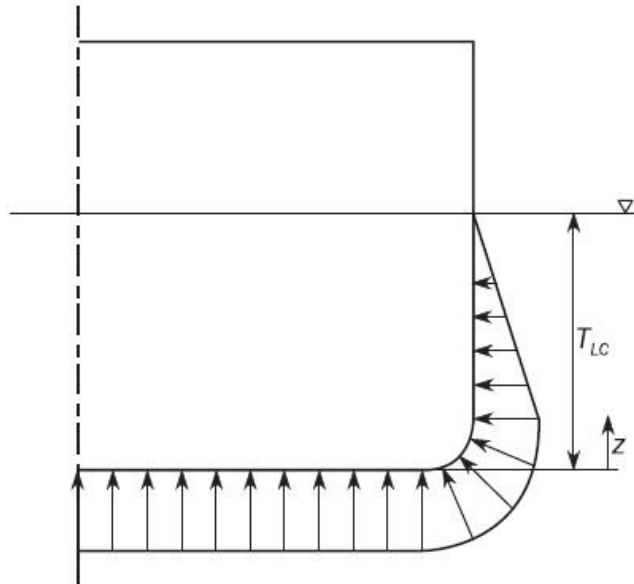
2.3, and see figure 2.5.

Figure 2. 5 Hydrostatic pressure

Location	Hydrostatic pressure (P_s)
$Z \leq T_{LC}$	$\rho g(T_{LC} - Z)$
$Z > T_{LC}$	0

Table 2. 3 Hydrostatic pressure

Wave pressure

We calculate the wave pressure base on the hydrodynamic pressure for HSM, FSM,BSR and BSP load cases, detail calculation process, please refer to [70].

c. Bottom slamming pressure

Relative acceleration between the ship bottom and a wave can produce a violent slamming pressure. we often apply the follow two cases to assess the bottom slamming design load.

Case 1: An empty ballast tank or a void space in way of the bottom shell.

Case 2: A full ballast tank in way of the bottom shell.

Case 2 is considered as its ultimate load cases in this study.

To guarantee structural design reliability of the SP, all dynamic load conditions should be considered in the optimization process. The dynamic load conditions can be connected through load combination factors as explained in the CSR. Load cases above mentioned are connected through the working-case weighting factor ω_k, which will be talked in section 2.3.

2.2 The current development of stiffener layout optimization method

Over the past few decades, a variety of methods based on topology optimization have been developed to predict the optimal layout and/or size of stiffeners used to strengthen the plate or shell structure. Having the proper stiffeners distribution on a shell structure can improve its structural dynamics, stability, and static performance [37]. There are two main method to generate stiffener until to now, which will be described in the following part.

2.2.1 Ground structure method

this way involves discretizing a plate-beam structural model (ground structure method), in which a large amount of stiffeners are pre-established in the structure. This method searches for the optimal stiffener layout by controlling stiffener growth and fade based on growth theories and a TO method.

The ground structure method is put forward by Dorn et al[71], and widely applied in topology optimization of trusses. Oberndorfere[72] suggest using discrete elements to generate stiffeners. Liu and Yan[73] proposed a discrete method for generating

automobile stiffeners. Several design criteria have been taken into account in optimization, such as strength, stiffness and buckling. The idea has also been tested to optimize the location of stiffeners on aircraft frames. Although the optimization results prove that this method is simple and effective, the optimality of this method depends on the initial ground structure. In order to obtain satisfactory results, the ground structure should be constructed as densely as possible, limiting its application in the design of large machine tools. When the layout of the stiffener layout is complicated and the tendons are oriented in any direction, it is also very difficult to analyze the problem.

2.2.2 Thickness distribution method

This method, based on the optimal thickness distribution, uses stiffener generative theory to transform the problem of stiffener-layout design into that of optimal material layout, this approach intends to find an optimal stiffener layout within a given design domain for specified objectives and boundary conditions, which is the more commonly applied in practical design.

Krog et al.[74] used that approach based on the SIMP method to obtain new and better fixed leading-edge stiffeners and fuselage-door intercostal. Wang et al. [75] used the same approach based on the subset method to design a new stiffener layout for an aircraft wing, making the stiffeners lighter than the originals. This method also be used in the submarine sail structure, the results show that the total stiffener weight reduced by 19% compared with the original model[44]. There have been many other successful stiffener-layout optimizations that have adopted this approach [76, 77].

Meanwhile, some other stiffener-generating methods have been proposed as follows.

Motivated by the growth mechanism of branching systems in nature, Ding and Yamazaki [78] proposed a bio-inspired method known as the adaptive growth method. Bojczuk and Szteleblak [79] proposed a heuristic way to find an optimal stiffener layout. And both of these methods got better structural performance.

The aforementioned examples of stiffener layout optimization are based on two-dimensional (2D) structures. However, there are also some successful examples involving three-dimensional (3D) models [80, 81], the optimization processes are more complex than for 2D optimization.

Strictly speaking, the design of stiffeners obtained from topology optimization is only the approximate value of material layout in topology optimization. In order to solve the difficulties in the numerical description for stiffeners, the focus of early papers is to consider the design of stiffeners as the thickness design of solid or shell elements.Such as, Cheng and Olhoff [82] maximized the stiffness of rectangular and axisymmetric plates with the help of a thickness distribution optimization, which was the original form of topology optimization. This idea was later extended to the stiffener layout design applied in composite materials[44]. Besides, In order to improve the precision, the casting constraints can be applied in topology optimization. it is used to design the stiffener layout, in which the material distribution along the specified direction must meet certain manufacturing requirements, such as casting, milling, forging etc.

As for some manufacturing constraints that this paper adopts, which will be described in the section2.3.3.

2.3 Layout optimization design

2.3.1 Optimization mathematical model

At present, the research of continuum structure topology optimization are mainly concentrated on single objective topology optimization, as describe in the reference in [83, 84]. Actually, due to the complexity of structure condition, a single objective optimization method is difficult to comprehensively consider each working condition, only a single objective topology optimization is hard to achieve the optimal structure which meeting the needs of actual engineering. then the multi-objective topology optimization method considering various conditions was put forward. Such as, Fan et al, focused on the frame studied the multi-objective optimization, static stiffness and dynamic vibration frequency taken as objective[85]; Lin et al, use Optistruct software to optimize a SUV frame and achieved the structure meeting the requirement of stiffness and vibration frequency[86]; Jiang et al, successfully got the optimized structure of dump truck frame through multi-objective optimization[87]. Jiang also apply this optimization method to optimize the U-type platform, its quality reduced, stiffness increased, natural frequency meet the requirements[88]. The examples above all are the successful applications of multi-objective topology optimization, and applied in practice. Which prove that it is feasible to apply multi-objective topology optimization. So, this paper presented a multi-objective topology optimization method for ship prow stiffener, in which both compliance and eigenfrequency were regarded as static and dynamic optimization objectives, based on SIMP method. Detail multi-objective topology optimization will be introduced in the following,

Natural frequency topology optimization function

Natural frequency topology optimization can maximize the frequency which can help structure avoid or higher than vibration frequency and prevent the occurrence of resonance phenomena. In the process of structural frequency optimization, if only the first order frequency as the optimization goal, when it becomes max, several other frequencies will be reduced to a lower value, the frequency aliasing phenomenon occurs. So, in this paper, the mean frequency optimization function was applied [89]. this function can define a smoother objective function, the objective function can keep smooth even if several low order modes frequency exchange during optimization process. This function is described as follows:

$$\max f(\rho) = f_0 + \alpha \left(\sum_{i=1}^{m} \frac{\omega_i}{f_i - f_0} \right)^{-1} \tag{2.3}$$

Where, f_0 a given initial frequency, m stands for the largest order of frequency, ω_i is the given weight coefficient. α and f_0 are all given arbitrary constants which are only used to make physical meaning of the objective function and adjusting the dimension of the objective function $f(\rho)$. In this equation, we set $f_0 = 0$, $\alpha = \sum_{i=1}^{m} \omega_i$, because we calculate the mean frequency value of the first six order frequency and assume the weight factor of each order frequency is equivalent, so the $\omega_i = 1, \alpha = 6$.

Stiffness topology optimization function

Stiffness topology optimization is to maximize the stiffness of the structure under constraints. The stiffness topology optimization based on multiple load cases is usually used as a multiple stiffness topology optimization stiffness[90]. Each load case corresponds to an optimal stiffness structure, different load cases can get different

optimal stiffness structure. So, the multi-stiffness topology optimization is considered as a multi-objective topology optimization. In this paper, a single objective optimization of stiffness cannot meet our requirements. In order to make the stiffness under various working conditions can be optimized, it is need to define a multi-stiffness topology optimization function. Compromise programming approach is applied to deal with multi-objective problem[91]. Besides so we used compliance response instead of stiffness. Then the function shows as follows:

$$\min C(\rho) = \left\{ \sum_{k=1}^{n} \omega_k^q \left[\frac{C_k - C_k^{min}}{C_k^{max} - C_k^{min}} \right]^q \right\}^{\frac{1}{q}}$$

(2.4)

Where, C stands for the compliance; n is the serial of the load cases, there are eight load cases; q is penalty factor, $q \geq 2$, in this study we set q value is 2; ω_k is the weight factor of load cases.

Multi-objective topology optimization function

To the U-type platform with electro-optic load, the stability of the structure is very important. So, it is meaningful to improve the stiffness and natural frequency. In order to realize the optimization of stiffness and natural frequency at the same time, the idea of the compromise programming method was applied which can harmoniously combine natural frequency topology optimization function and stiffness topology optimization function. And the volume fraction as constraints. Then the objective function shows

$$\min F(\rho) = \left\{ \omega^2 \left[\sum_{k=1}^{n} \omega_k \frac{C_k - C_k^{min}}{C_k^{max} - C_k^{min}} \right]^2 + (1 - \omega)^2 \left(\frac{f_{max} - f(\rho)}{f_{max} - f_{min}} \right)^2 \right\}^{\frac{1}{2}}$$

$$s.t. \qquad \sum_{m=1}^{M} \rho_n V_n \leq V_0 \qquad n = 1, 2, ... M \tag{2.5}$$

$$0 < \rho_{min} \leq \rho \leq 1$$

Where, $F(\rho)$ is the multi-objective function value; ω is the weight factor of compliance function. We set ω value is 0.5; volume ration is 0.3.

2.3.2 Manufacturing constraints

To ensure a reasonable stiffener layout, manufacturing constraints should be considered during the TO process. There are following manufacturing constraints are considered:

a. Casting constraints

Cavities that are not open and lined up with the sliding direction of the die are not feasible during optimization process, Designs obtained by topology optimization often contain cavities that are not viable for generating stiffener. To ensure a reasonable stiffener layout are built based on the reason given above, casting constraint is considered, which can avoid cavities being generated inside the structure. The mathematical formulation of the casting constraints based on pseudo-density is as follows:

$$(0 \leq \rho_i \leq \rho_j \leq ... \leq \rho_n \leq 1)_k \quad k = 1, ... K \tag{2.6}$$

Here, $\rho_i, \rho_j ... \rho_n$ represent the pseudo-densities of elements along the same line in the casting direction as shown in Figure 2.6, K is the number of sets of elements in the draw direction, and n is the number of elements in a row. On account of equation 2.6, the cavities inside the structure have to be open in the casting direction of the die and all exterior and interior boundaries have to keep the signs of their slopes relative to the casting direction unchanged.
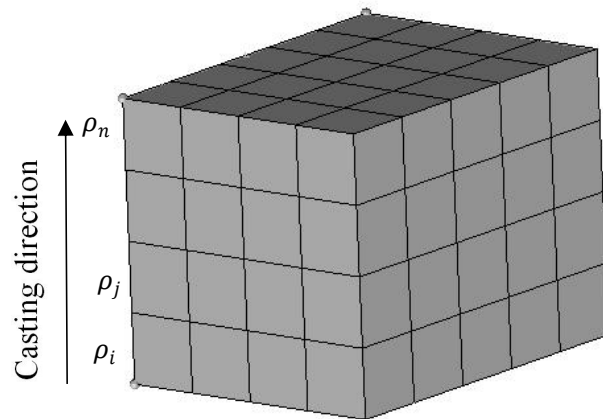
45

Figure 2. 6 An illustrate FEM with a prescribed casting direction

The effect of the optimization result within the casting constraint is shown in figure 2.7 (http://www.altairhyperworks.com/product/OptiStruct） shown, in which there are no cavities and material barrier are generated. The result proves that the manufacturing constraint is suitable for generating a stiffener in a solid structure.
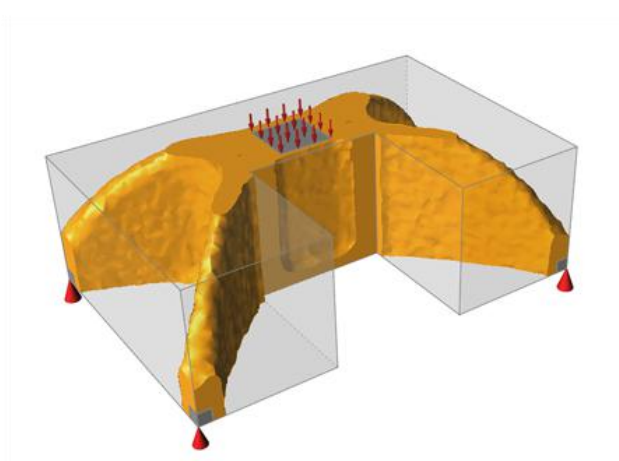
With casting constraints
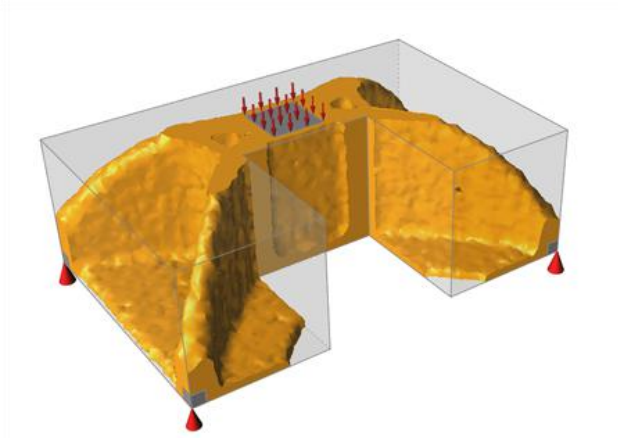
Without casting constraint

Figure 2. 7 Optimization result (casting constraint)

Then the equation 2.6 can be modified based on equation 2.5, The TO problem under casting constraints can be formulate as follows:

$$\text{Min } F(\rho)$$

$$\sum_{m=1}^{M} \rho_n V_n \leq 0.3 \qquad n = 1,2….M \qquad (2.7)$$

$$(0 < \rho_{min} \leq \rho_i \leq \rho_j \leq …\rho \leq \rho_n \leq 1)_k \;\; k = 1,2…. K$$

b. Symmetry constraints

Planar Symmetry is applied during optimization process in this paper, which can avoid disordered accumulation of materials effectively, which can make the stiffener layout more reasonable.
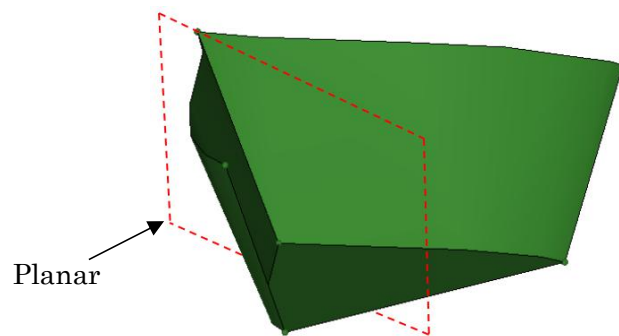

Planar

Figure 2. 8 Planar symmetry

c. Member Size Control

●Minimum Member Size Control

The minimum member size is the minimum scale allowed in the density area of 1, which can eliminate the smaller load-transferred path during optimization process, thereby a more uniform distribution of materials can be obtained. We set the minimum member size is at least 3 times the average element size.

●Maximum Member Size Control

Maximum member size control is used to punish the formation of large members. Which can eliminate the accumulation of materials during optimization process. the control is not directional, this means that if the member thickness is smaller than maximum member size, the constraint condition is satisfied. this reflects the need to control the stiffener thickness of casting parts.   The maximum member size is at least twice minimum member size.

2.3.3 Optimization algorithm

In the TO stage, we adopt a sequential quadratic programming solution algorithm, which is a gradient-based optimization algorithm that is suitable for solving TO problems. This algorithm finds solutions of constrained nonlinear optimization problems. The aforementioned objective function and constraint function are linked together by Lagrange multipliers as follows:

$$L(x,\mu_1,\mu_2) = f(x) + \mu_1 b(x) + \mu_2 c(x). \qquad (2.8)$$

Here, $f(x)$ is the objective function, and $b(x)$ and $c(x)$ are equality-constraint and inequality-constraint functions, respectively. Terms μ_1 and μ_2 are Lagrange

multipliers, which can be solved for using the Kuhn-Tucker condition [92]. Here, the optimization problem can be simplified as equation 2.7.

2.4 Layout optimization results

2.4.1 Challenges of generating a topology layout

A. objective function selection

the most common objective of density method is to minimize the compliance(maximize its stiffness) based on the required constraint material function[19]. This material constraint function can be expressed in terms of the absolute volume target or the volume fraction for the initial design space. This formula does not represent typical engineering design problems, because typical engineering design problems are often related to stress, displacement and buckling constraints. However, we can apply it effectively for visualizing material placement and the best loading path. In addition, the design of stiffeners based on topology optimization with minimization compliance objectives maybe perform well under constraints such as displacement and stress[21]. The SIMP method often uses other optimization models, such as minimizing the mass and frequency to achieve constraint displacement, which can be directly applied to engineering design cases[93, 94].

Multi-objective topology optimization method is applied in this paper, which is seldom applied in the actual application, its accuracy and efficient are not be discussed in the previous article, put the equation which not existed function in software into the Optistruct by ourselves. Optistruct uses linear finite element analysis and gradient based optimizer to solve this multi-objective function problem.

In summary, this paper also presents challenges to other goals other than the objective

function.

B. Parameter effect

Baseline topology

the high-density region (the red area shown in the figure 2.9) represents the baseline. The penalty factor P that we used is 0.3 for filtering the checkboard phenomenon and avoiding the numerical problems have a bearing on linear element formulas. in this case, we set the volume fraction is 0.3, which is a common initial value. The optimization contour can be applied to potential stiffener position or initial concept stiffener. But the optimization parameter can affect the layout problem evidently
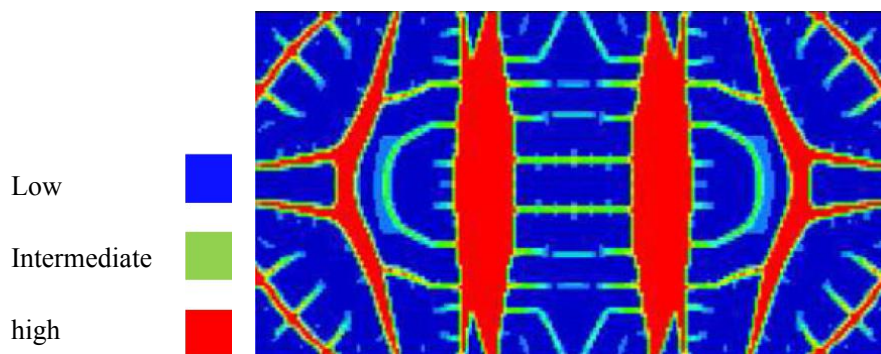
Figure 2. 9 Topology baseline layout

Effective of volume fraction

Volume fraction is an important optimization parameter for the generation of stiffeners based on topology optimization. when the VF less than 15%, the contour plot cannot show clear and constant stiffener pattern like the higher VF(25%); and when the VF more than 40%, the material distribution begins to accumulate[95].

The sensitivity of loading path makes it difficult to determine which layout is the best, because they are locally optimal, and their real performance and behavior are still

unknown until interframe capture and size adjustment steps. Therefore, the volume fraction is an important optimization parameter to find the optimal layout of stiffeners based on the pressure plate.

C. Interpretation challenges

This challenge is about how to generate a feasible stiffener layout from the topology layout results, because it needs the engineering judgement and knowledge. The first step about explaining the layout is to determine the location of the stiffeners. The location of primary potential stiffeners is often determined by observing high-density elements, which often emerge in the initial steps of topology optimization, it can be seen from figure 2.10. in general, the primary stiffener can resist the global structure deformation.
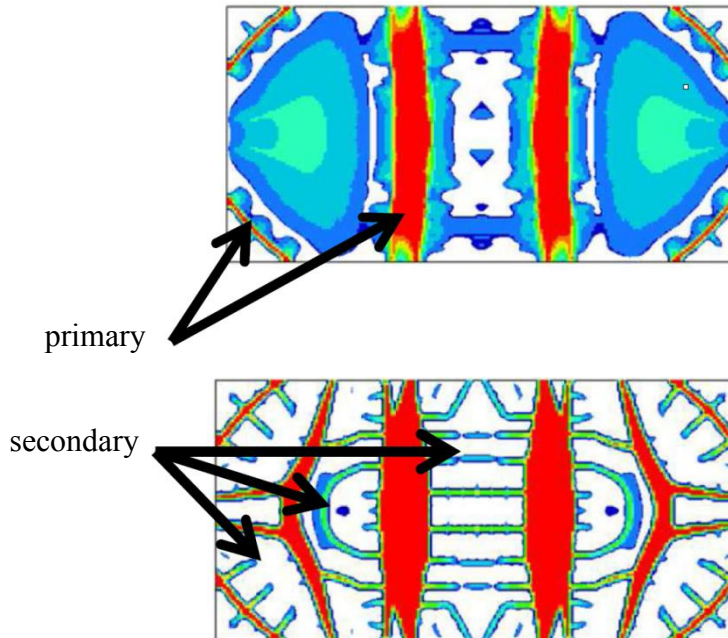
Figure 2. 10 Stiffener position interpretation

The lower density member is often considered as secondary stiffener, these results are

appeared in the later iteration steps. Secondary stiffeners are used to minimize the structure compliance by means of supporting the bay generated based on primary stiffeners. they combine all the design spaces together fully and indirectly help improve the mechanical properties of the main reinforcement. So, we can interpret the high and low-density members as potential stiffeners, but it is controversial to retain low-density stiffeners for direct interpretation.

The stiffener locations are sensitive based on optimization parameters, making it hard to prove that these stiffeners locations are accurate. And many of stiffeners come from primary members and there are no obvious influences for loading path.

In conclusion, low density characteristics may have less important for generating initial stiffeners design concepts, but maybe it is necessary for handling bay support in subsequent steps.

2.4.2 Optimization analysis

In this paper, we utilize the aforementioned manufacturing constraints, adopting a 3D model to optimize the stiffener layout according to some successful cases in generating stiffeners based on 3D models, these cases show that applying appropriate manufacturing constraints in 3D topology optimization can make the solid elements equivalent to a design space modeled with 2D elements.
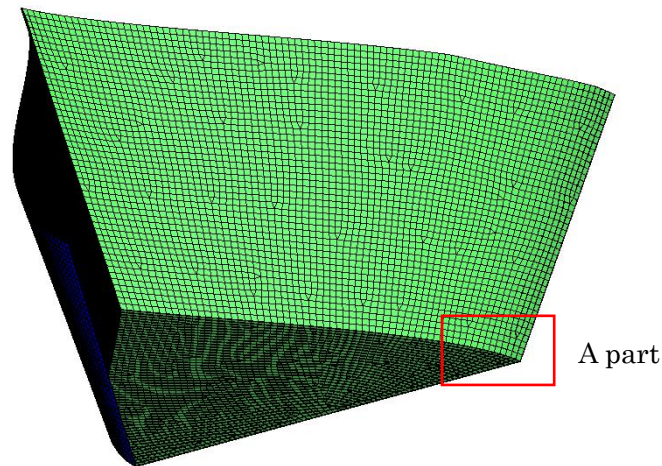
Figure 2. 11 Finite element analysis model

The aim at this stage is to obtain the optimum distribution of material under the prerequisites of obtaining the minimum compliance and maximum eigenfrequency.

Finite element model construction

According to shipbuilding design rules and actual ship skin thickness, we assume the thickness of ship prow skin is 28mm, we considered ship prow shell as non-design region, which means that this part will not change during optimization process. And assume the thickness of design area is 120mm, its thickness is thicker than the actual thickness of ship prow. because we don't know the actual thickness, so we set the thickness as thick as possible. Thus, not only can we get the reasonable material distribution layout, but also can get the stiffener height indirectly.
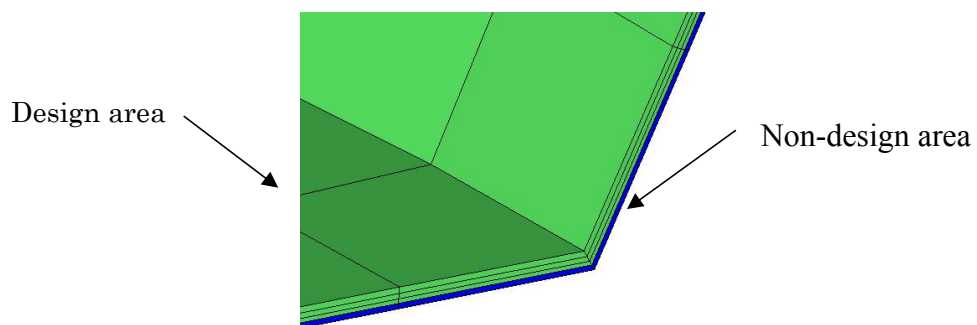

Figure 2. 12 Local FEM model (A part)

As figure 2.11 and figure 2.12 shown, the blue area represents the non-design area, the green area represents the design area.

The material which the ship prow adopts is mild steel Q345, its performance parameters are shown in the following table 2.3.

Yield strength (σ_{max})	*345Mpa*	Density (ρ)	*7850Kg/m³*
Young's modulus(*E*)	*206GPa*	Poisson ratio	*0.3*

Table 2. 4 The performance of mild steel

Boundary condition

The load cases that we adopt is from section 2.1, With regard to Equation 2.6, we set $\omega_k = 1$, meaning that every load condition is equivalent for the compliance objective function, and $\omega = 0.5$, meaning that the compliance and eigenfrequencies are equivalent for the synthetic objective functionF(ρ).

According to section 2.4.1 explanation, the volume fraction ratio that we take is 0.3, this ratio is beneficial to get a clearer material distribution, and this ratio is also better for us to find the exact position of the potential stiffeners. Besides, the manufacture constraints which mentioned in the section 2.3.2 are all adopted.

Optimization results

convergence criterion

Regular convergence criterion is adopted, this means that for two consecutive iterations, if the change in the objection function is less than the objective tolerance, then the optimization stops. Mathematical model can be expressed as below,

$$|f(x_{i+1}) - f(x_i)| \leqslant a \qquad (2.9)$$

In this paper, the convergence criterion value a is 0.005.

Optimization results analysis

The optimization process stopped after 32 iteration steps, the convergence criterion value a is 0.003 less than prescribed value 0.005. the iterative process curve is shown as figure 2.13. this figure shows that the objective function tends to be smaller with the increase of iteration steps.

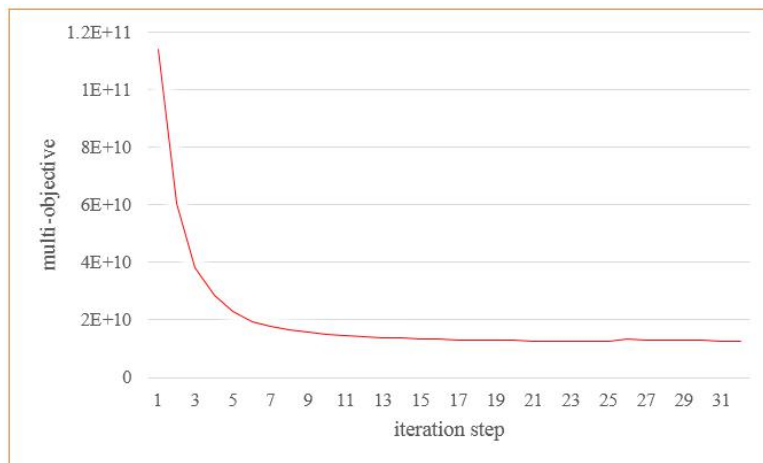Figure 2.14 shows the volume change(VCR) rate with the increase of iteration step, the VCR also tends to be smaller.

Figure 2. 13 Iteration step of objective function
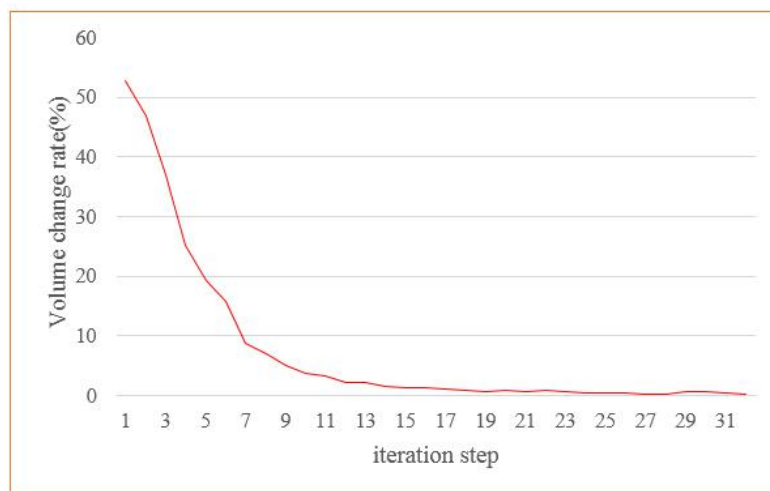

Figure 2. 14 Iteration step of volume change rate

Form figure 2.13 and figure 2.14, we can make a conclusion that volume change rate and multi-objective function have a positive correlation with the convergence criterion, conforming to the optimal design criteria

The optimization results corresponding to some iteration steps are shown in the following figure 15,

Iteration 3
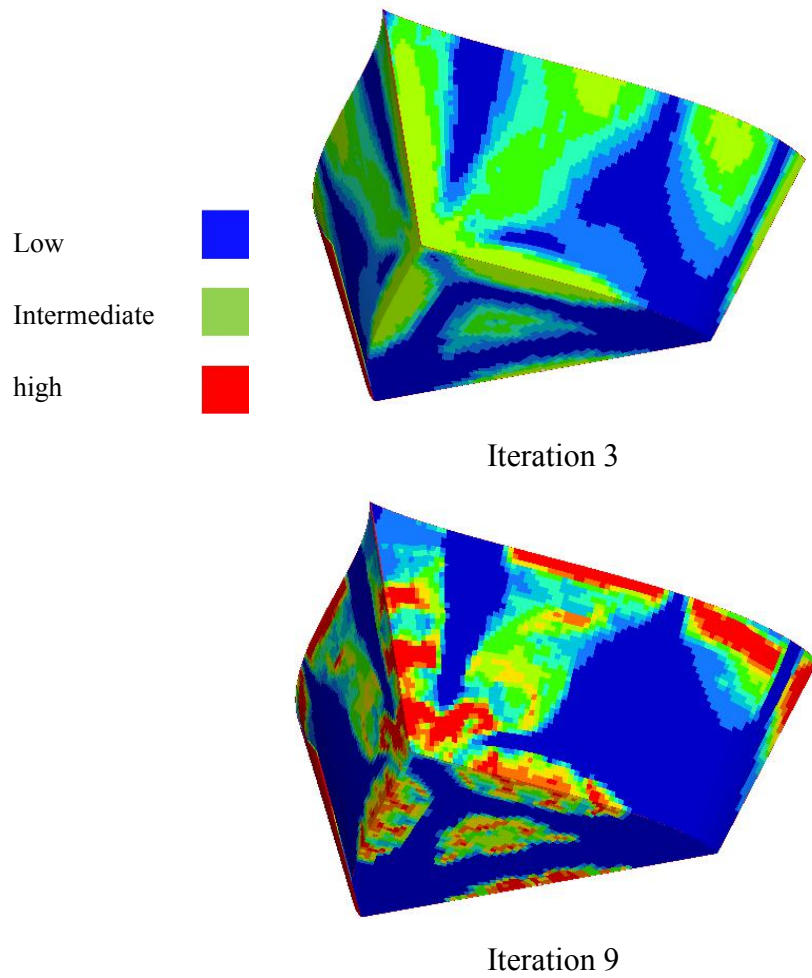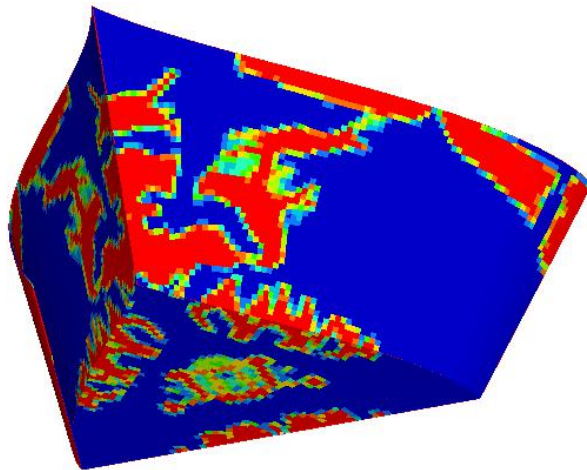
Iteration 9
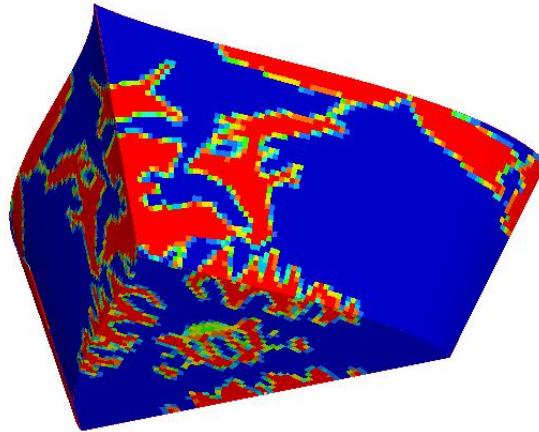
Iteration 25

Iteration 32 (Final)

Figure 2. 15 Stiffener position interpretation

From the four representative layouts are specifically retained in figure 2.15 we can know the contours of material layout become clearer; the potential primary stiffener position is gradually determined. Although minimum member size control punishes the small members to be generate, the results still show that many smaller size members can be generated than the specified minimum member size. Because these smaller stiffeners play an essential role for the load transfer and cannot be eliminated through penalization factor. Blue regions represent low material density, red regions represent high material density (whose density threshold $\rho \geq 0.3$). There are no cavities and

material barrier are generated, the material distribution range is reasonable, vertically-walled stiffeners of variable heights based on manufacturing process in the optimization result. These contours are used to determine a design with optimal load paths. Regions with low material density are deemed to be holes, which represents the material can be removed.

To make it easier to observe the potential stiffener position and height, the structure with these holes removed is shown in the figure 2.16.
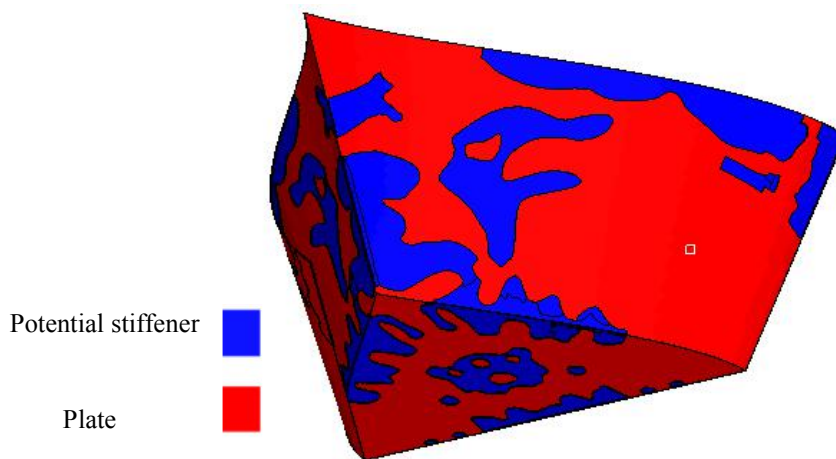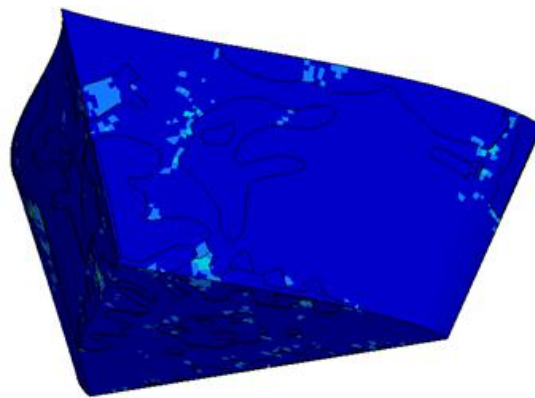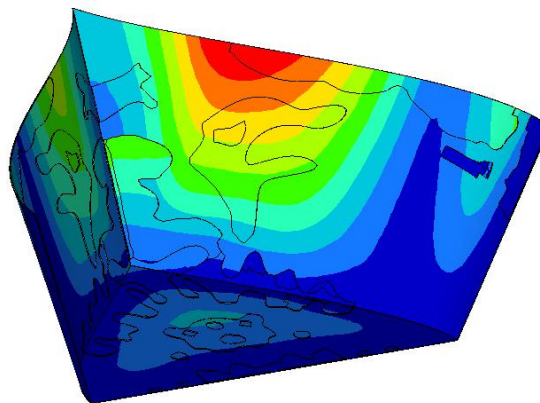

Figure 2. 16 Potential stiffener layout

Regions with high material density are where the structural rigidity requires strengthening. The combined weight of these high-density areas is 36.2 ton, which can be considered as supporting the global deformation of the structure and minimizing the total compliance. Hence, these areas can be interpreted as a potential stiffener model by the designer.

In order to verify the effectiveness of the stiffeners, we carry out finite element analysis on this potential stiffener model based on the above-mentioned load cases, the analysis results corresponding to the maximum load cases as following figure 2.17 shown, the structure is subjected to a maximum stress of 279.4 Mpa, which located in

the junction between side shell and bottom, except here, there is no larger stress exists, and the stress which the whole ship prow subjected is equilibrium; the maximum structural deformation is 1.397 mm, which locate at the top of side shell, which within one percent of the longest dimension of ship prow structure, the deformation value is within the allowable range; and the first-order frequency is 0.435 Hz.

Stress contours

Displacement contours

Figure 2. 17 Analysis results for potential stiffener configuration

The analysis results prove that stiffeners layout based on topology optimization within manufacturing constraints are reasonable, this method can improve structure performance while reducing material.

Because curved stiffeners as shown in Figure2.16 are difficult to produce, we should

instead arrange regular stiffeners in the high-density areas as far as possible. In the next section we will talk about it.

2.5 Feasible stiffener layout

Curved stiffeners are difficult to produce, so we should adopt a suitable stiffener style whose mechanical properties can satisfy the requirements of use to replace curve stiffener. we should arrange suitable stiffeners in the above high-density areas based on topology optimization results, stiffener theory and stiffener construction rules in shipbuilding, keeping the skin thickness as 28 mm.

there are a lot of styles of stiffener can be chose in engineering application. In this paper, T style stiffener is adopted in this thesis, because this type of stiffener has a satisfactory moment of inertia, this type of stiffeners is conducive to the high bending load that are generated by the pressure from plate shell. thereby decreasing structural deformation[96, 97]. Detail stiffener section as figure 2.18 shown, there are four dimensional parameters will be conducted to size optimization in the following chapter, they are web plate length(L), web plate thickness (t_w), wing plate length (L_f), wing plate thickness (t_f).
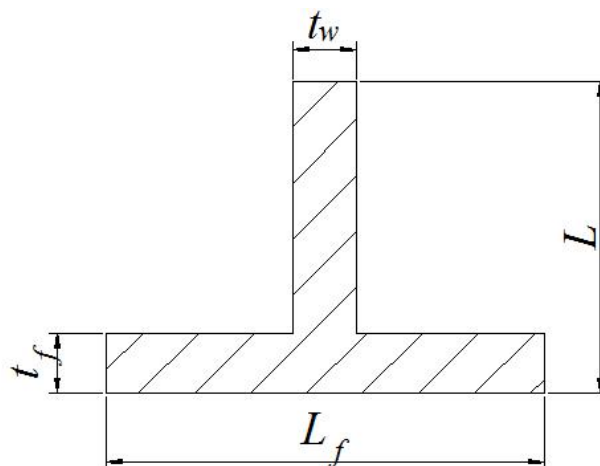

Figure 2. 18 Stiffener type

To maintain as much structural compliance and weight balance as possible after arranging the stiffeners, the initial stiffener location and size should be considered according to the actual high-density areas and the stiffener design rules of shipbuilding. the initial stiffener location and size should be considered according to the actual high-density areas and the stiffener design rules of shipbuilding[98]. The appropriate transverse and longitudinal intervals are 1,000 mm and 850 mm, respectively, along the side of the ship, and 750 mm and 800 mm, respectively, along its bottom. The initial stiffener dimensions are given in Table 2.5, with the total stiffener weight equal to the potential stiffener weight.

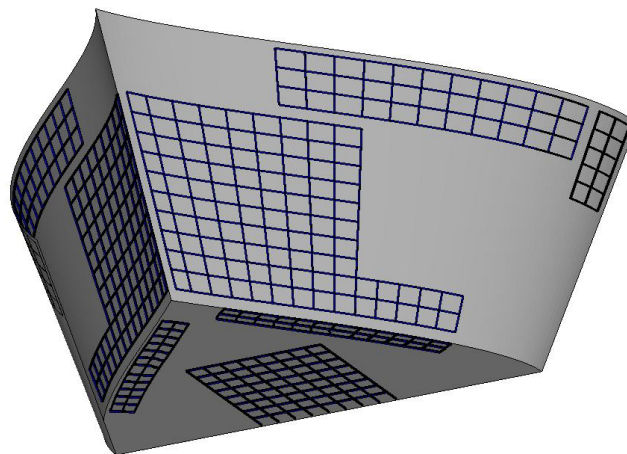| Height (L)	120 mm	Width (L_f)	110 mm
Thickness (t_f)	23 mm	Thickness (t_w)	25 mm

Table 2. 5 Initial stiffener dimensions

Figure 2. 19 Initial stiffener layout

Another difficulty arises in constructing a geometrical model. The SP surfaces are irregular curved surface, so to guarantee calculation accuracy and stiffener continuity in one direction, we need to establish the normal vector at each node and construct

numerous displacement coordinate systems. We must also connect the shell elements together with beam elements through the nodes. The initial layout of the stiffener structure in the SP is shown in Figure 2.19; the initial skin and stiffener weights are equal to the potential skin and stiffener weights respectively. Detailed patterns of node connection are shown in Figure 2.20.
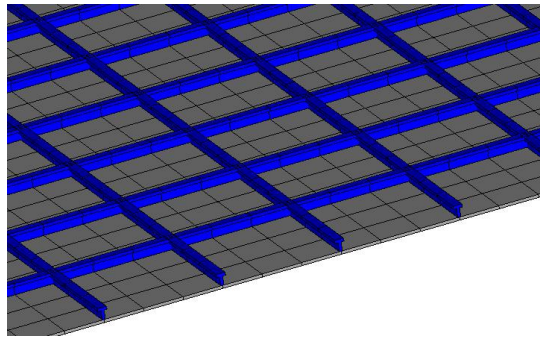

Bottom plate
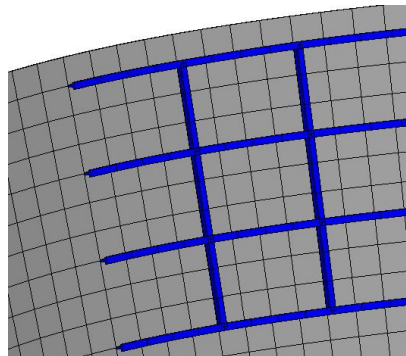
Side plate

Figure 2. 20 Conjunction of nodes

2.6 Performance estimation

We then carry out analysis for the initial stiffener model as shown in Figure 2.19, The structure is subjected to a maximum stress of 298.2 Mpa, the maximum stress locates in the connection between side shell and bottom; the maximum deformation is 1.484 mm, which located in the upper part of side shell; and the first-order frequency is 0.376

Hz. We find that the mechanical performance of the initial stiffener model is lower than that of the potential stiffener model. The detail analysis results of initial stiffener are shown in the figure 2.21.
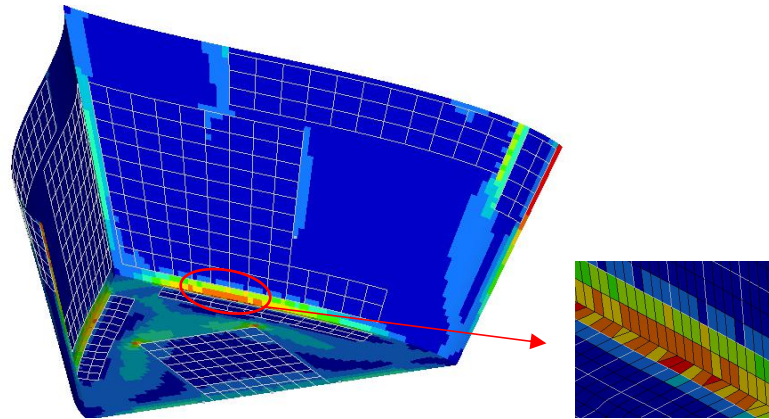
Stress contours
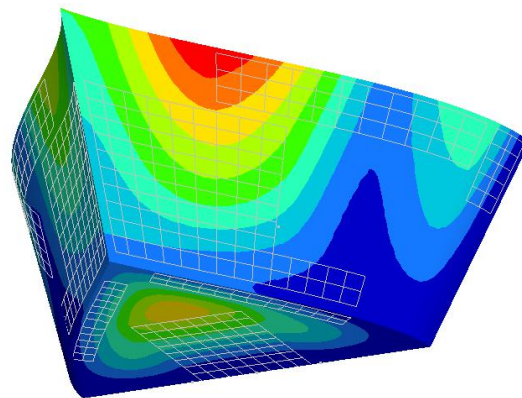
Displacement contours

Figure 2. 21 Analysis results for initial stiffener configuration

To improve the utilization of materials, later size optimization is conducted to optimize the initial stiffener model.

2.7 Summary

In this chapter, we introduce the research objective and its complex load cases for this paper firstly, and explain how to connect these complicated load cases together by

influence factor; secondly, introduce the two kinds of methods (ground structure and optimal thickness distribution) about stiffener design layout, after comparing the difference between them, the method of optimal thickness distribution is adopted to find the optimal stiffener layout; then taking multi-objective function (stiffness and eigen frequency) as optimization goal and optimize the ship prow based on some manufacturing constraints, getting a reasonable material distribution(potential stiffener), but it is hard to be produced, so we construct a regular stiffener based on optimization results and shipbuilding rules to replace the potential stiffener (curve stiffener).

Chapter 3

Stiffener size optimization

Size optimization is generally performed after topology optimization to improve the concept design, interpreted from topology optimization[39, 99], to best performance. The process of size optimization can be seen in follow figure 3.1.
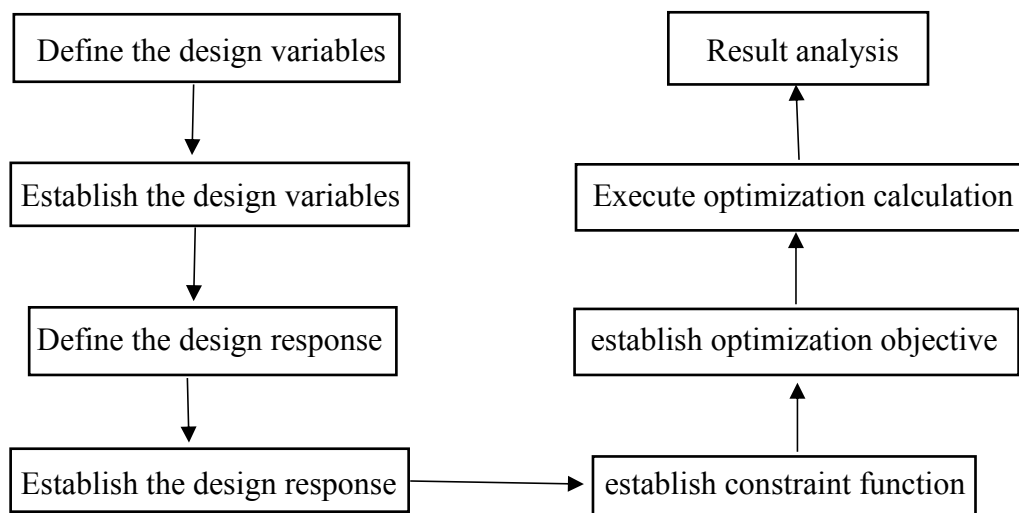

Figure 3. 1 Flow chart of size optimization for SP

3.1 Selection of the design variables

The following aspects should be paid attention before we select design variable:

▲ The choice of design variables must have an impact on the objective function. But if the selected design variables have great influence on other performance, these design variables cannot be selected.

▲ the numbers of selected design variable should be controlled. If the number of design variables is excessive, this will increase the computation time or the possibility

of the result non- convergence. If the numbers of design variables are fewer, the design effect of size will not be ideal, need to conduct size optimization again.

▲ the range value of design variables should be reasonable and need to meet the actual situation of the engineering project.

The aim of this stage is to optimize the plate shell thickness and stiffener cross section simultaneously to minimize the structural mass. So, there are five design variables are defined in this size optimization stage, for the stiffeners, the design variables are web plate height (L), web plate thickness (t_w), wing plate length (L_f), wing plate thickness (t_f), which are shown in the figure 2.18; besides the fifth design variable is the plate shell thickness.

We pay close attention to the skin and stiffener design-variable ranges prior to size optimization, constructing a reasonable parameterized model to avoid producing invalid dimensions. The parameter relationship between the shell plate thickness and the stiffener dimension is expressed as follow equation,

$$L_{\text{wmax}} = 2L_{fmax} = 10t_{wmax} = 10t_{fmax} = 10t$$

$$t_f - L < 0$$

$$t_w - L_f < 0$$

(3.1)

Where, t is the basic shell thickness, ranging from 15 mm to 45 mm. For the meanings of the other terms in Equation 3.1, please see Figure 2.18. about detail size range, as table 3.1 shown.

Then we construct an associated parameter model that links the stiffener section dimensions and plate thickness as an objective function; the relational expression between stiffener and skin, please refer to equation 1.18. in that equation, we assume $C_0 = 0$, $IDV_i = 1$ so that each design variable affects the objective function equally.

Structure size	Dimension range	Initial value
Shell (t)	10~45 mm	28 mm
L_f	t~5t	110 mm
L	t~10t	120 mm
t_f	t~5t	23 mm
t_w	t~5t	25 mm

Table 3. 1 Structure size range

3.2 Size optimization mathematical model

The aim of this stage is to optimize the plate shell thickness and stiffener cross section simultaneously to minimize the ship prow weight. Because of the thin-walled structure of the ship, the structure is more likely to fail by buckling (elastic instability) than by plastic deformation. Because the most important effect of stiffeners is against buckling, we consider the buckling constraints here. The design philosophy does not allow buckling of the structure below the ultimate loads, so the buckling constraints for optimization are defined so that the buckling load factor in linear-eigenvalue buckling is greater than the ultimate load.

Hence, to avoid creating bucking state, in this study we consider a buckling constraint (in the form of a buckling factor, *BF*) in this optimization step. The mathematical model of size optimization can be formulated as follows:

$$Min \quad f(A_i, t) = M_1(A_1, A_2, ... A_m) + M_2(t)$$

$$\sigma_{max} - [\sigma] \leq 0 \tag{3.2}$$

$$n - BF \leq 0$$

Where, $A_1, A_2, ... A_m$ are the stiffener cross sections whose initial values are same; and

assuming every section cross value varies equally for saving computation time; m is the stiffener number; t is the plate thickness, M_1 is the total stiffener weight, M_2 is the plate weight, $[\sigma]$ is the allowable structural stress, and assuming the allowable stress is 310 MPa; n is buckling factor value, setting the buckling factor value $n = 1$.

3.3 Optimization algorithm

We use the method of feasible directions (MFD) to solve the size optimization problem. A search direction is determined based on the gradients of the objective function and critical constraints, and then a line search is performed along this search direction. The solution procedure of MFD algorithm as follows, given a feasible point X^k to search optimal point,

$$X^{k+1} = X^k + d^k s^k \qquad (3.3)$$

Here, d^k is the increment and s^k is the iterative search direction. The solution procedure stops when objection function value $f(X^{k+1}) < f(X^k)$.

3.4 Optimization results analysis

The size optimization process stopped after 17 iteration steps, the iterative process curve of ship prow weight, this figure shows that the objective function tends to be smaller with the increase of iteration steps, the objective function tends to converge.
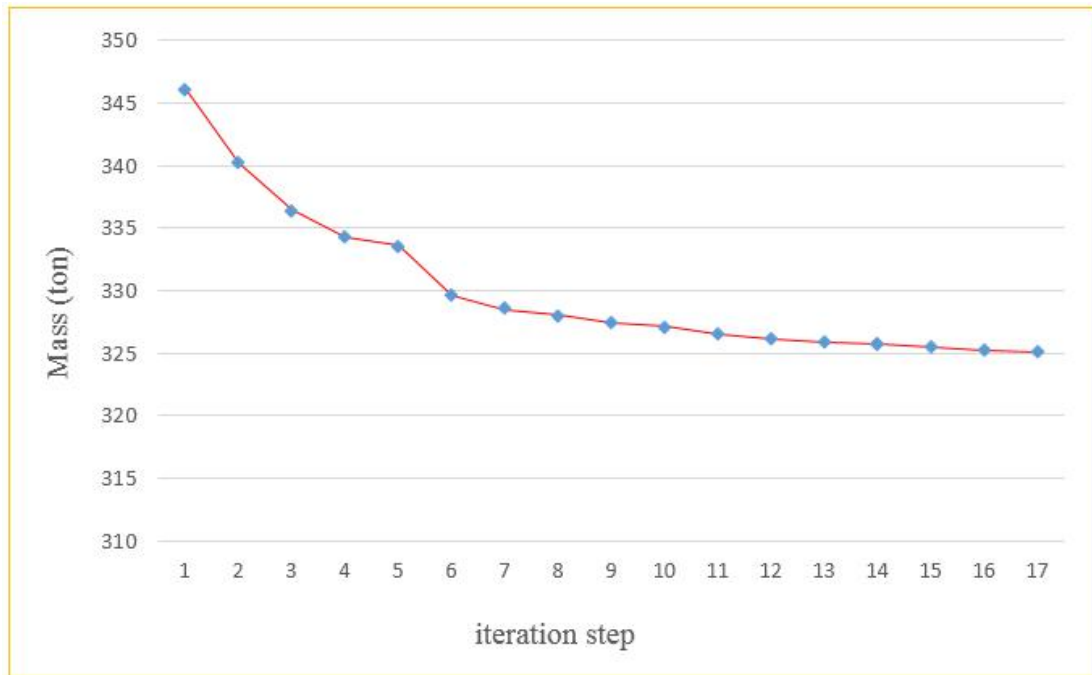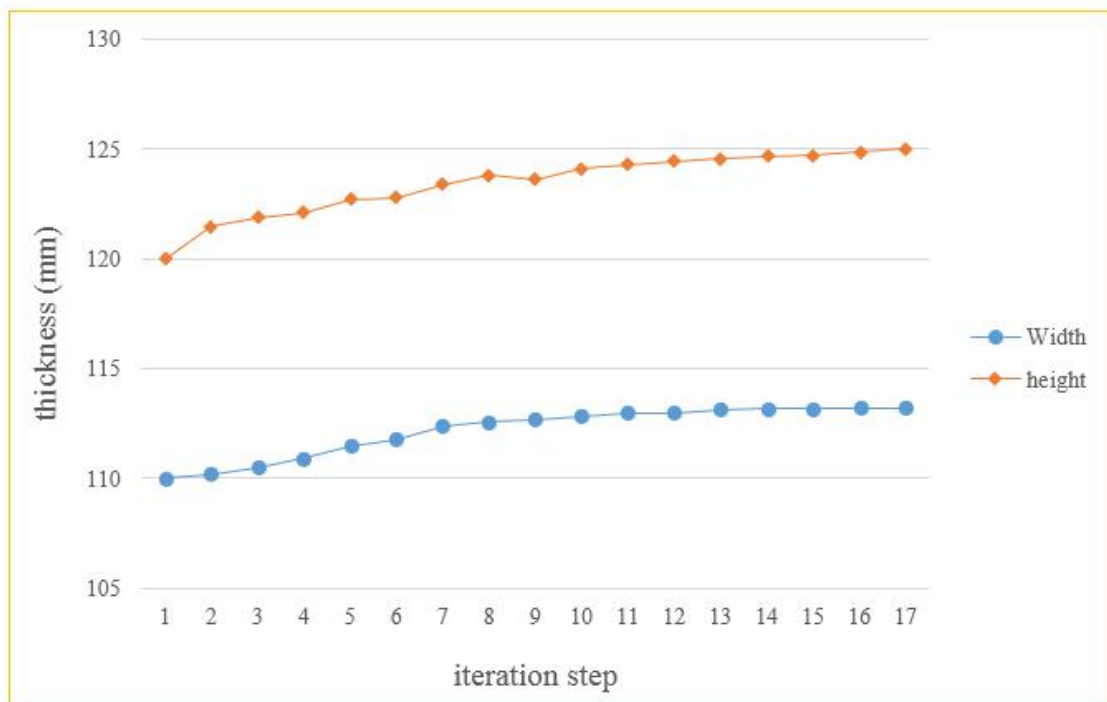
Figure 3. 2 The mass iterative curve

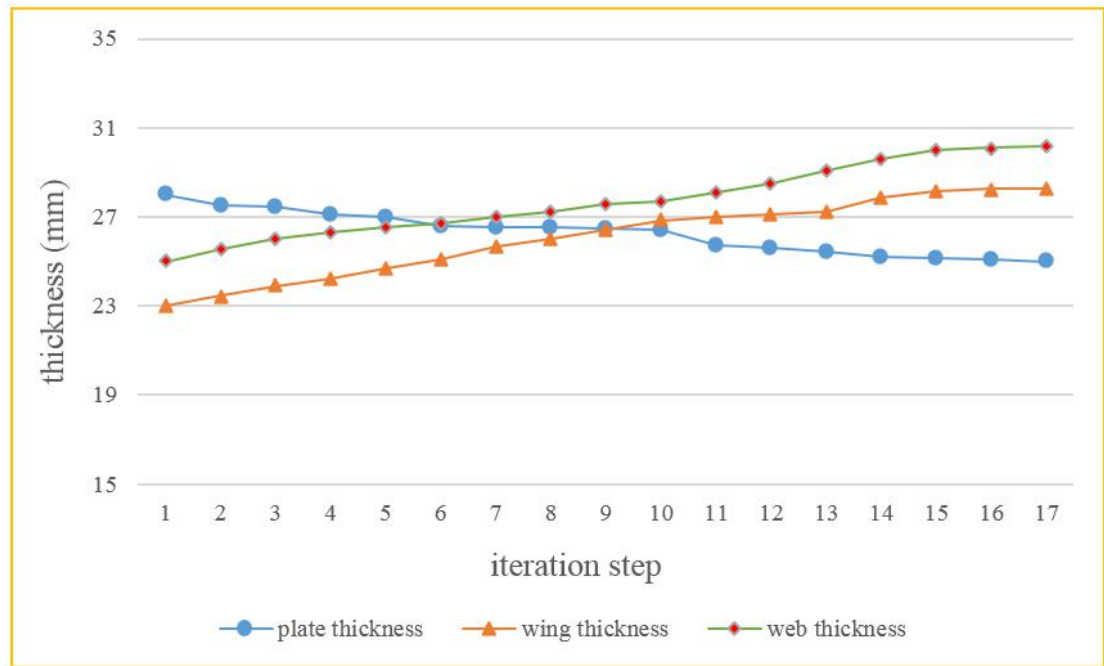Figure 3. 3 The height and width iterative step

69

Figure 3. 4 The thickness iterative step

From figure 3.3 and figure 3.4, we know that the design variables value of stiffener (L, t_w, L_f, t_f) become larger and the skin thickness intend to smaller with the increase of iteration steps.

The results of size optimization about design variable parameters are shown in the following table 3.2.

| Structure size	Dimension range	Initial value	Optimized value
Shell (t)	10~45 mm	28 mm	25.10 mm
L_f	t~5t	110 mm	113.20 mm
L	t~10t	120 mm	124.80 mm
t_f	t~5t	23 mm	28.30 mm
t_w	t~5t	25 mm	30.20 mm

Table 3. 2 Size optimization results

70

We construct a new model based on the size optimization results, and then carry out analysis to obtain the following results.

Figure 3.5 shows that the distribution area of the stress which the ship prow bears become more reasonable compared the previous stress results. And the maximum stress is 290 Mpa, the stress value is less than 310Mpa. The maximum deformation of 1.412 mm which located in the upper part of the ship's side as shown in Fig. 8. Furthermore, the first-order frequency is 0.416 Hz. All these parametric optimization results satisfy usage requirements, and the mechanical properties of the optimized stiffener model are better than those of the initial model. The stiffener mass increases to 47.26ton, skin stiffener mass reduces to 277.85 ton, and the total optimized model mass decreases by roughly 6% compared with the total initial model mass.
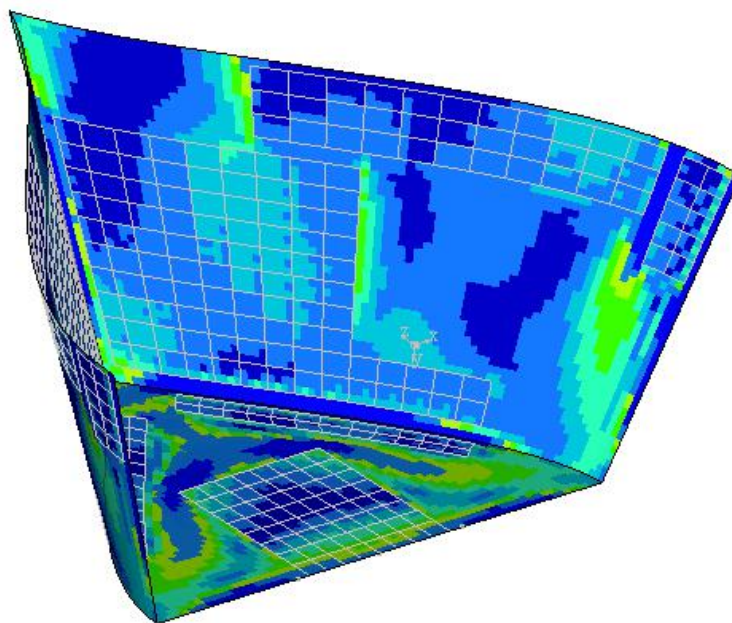
Stress contours
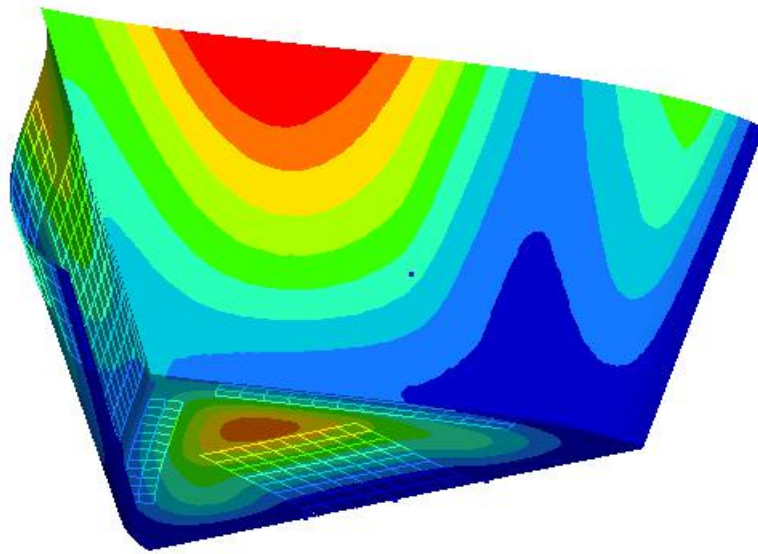
Displacement contours

Figure 3. 5 Analysis results for optimized stiffener configuration

In any practical application, it would be difficult to reproduce fractional values of the structural dimensions, so instead we round the optimized dimensions of the stiffener model to the values given in Table 3.3，

| Rounded stiffener dimensions			
Height (L)	125 mm	Width (L_f)	113 mm
Thickness (t_f)	28 mm	Thickness (t_w)	30 mm
Rounded skin dimensions			
Thickness (t)		25 mm	

Table 3. 3 Rounded dimensions of stiffener model

Then analysis the new finite element model again based on same boundary constraints, we obtain contours that are similar to those for the optimized stiffener model, because

the stiffeners size does not change greatly. That is because there is little change in the structural model dimensions, which leads to little change in the strain energy in the process of rounding.
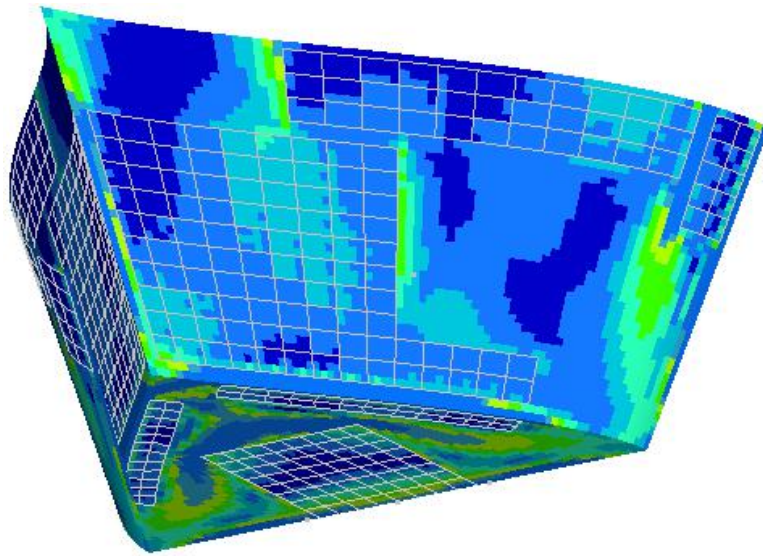
Stress contour
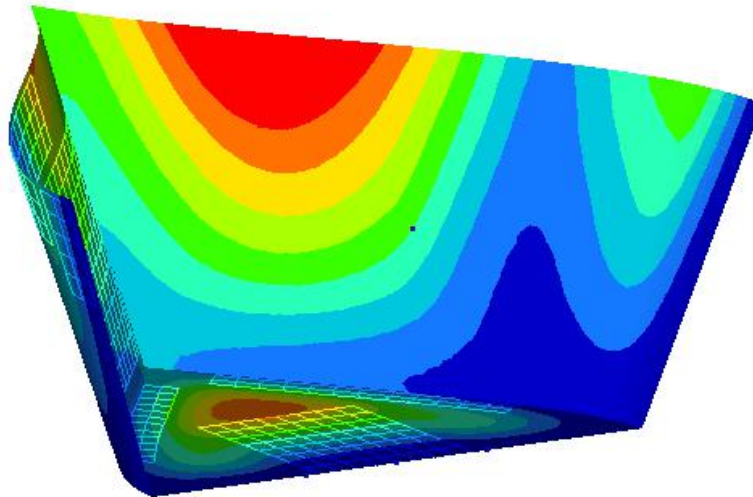
Displacement contour

Figure 3. 6 Analysis results for final stiffener configuration

The maximum stress that the ship prow bears is 291.6MPa, the maximum deformation

of 1.416 mm which located in the upper part of the ship's side. The final comparison results among these optimization schemes are shown in the following table.

Type Result	Potential stiffener model	Initial stiffener model	Optimized stiffener model	Final stiffener model
Stress	279.4 MPa	298.2 MPa	290 MPa	291.6 MPa
Displacement	1.397 mm	1.481 mm	1.412 mm	1.416 mm
Frequency	0.435 Hz	0.376 Hz	0.416 Hz	0.416 Hz
Skin mass	309.95 ton	309.95 ton	277.85 ton	276.74 ton
Stiffener mass	36.20 ton	36.20 ton	47.26 ton	47.18 ton
Total mass	346.15 ton	346.15 ton	325.11 ton	323.92 ton

Table 3. 4 Comparison of parameter values among stiffener models

From the table 3.4 result, we find that the mechanical properties of the final stiffener model meet the material performance requirements. Meanwhile, the total SP mass is reduced by 6.42% compared with that for the potential stiffener model.

3.5 Summary

In this chapter, size optimization is conducted as the detailed design stage for ship prow stiffener layout based on topology optimization.

Firstly, there are five ship prow parameters as design variables are selected for size optimization stage based on some design variable criterion. in order to make the optimization results reasonable and have practicability, a series of variation range are given to these variables, besides the parameter relationships among these five design variable are set up which avoid producing invalid dimensions.

Secondly, the mathematical model of optimization is established, the minimum mass is set as the objective function, Because of the thin-walled structure of the ship, the structure is more likely to fail by buckling (elastic instability) than by plastic deformation, so buckling factor is set as boundary conditions. After several iterations, the final design variable values are all within the range of specified value and the design variables change smoothly, which can prove the final design variable values are reasonable,

Lastly, an analysis model based on size optimization result is built, then finite element analysis method is conducted on this model, the analysis results prove that the size optimization is reasonable stage for ship prow; in any practical application, it would be difficult to reproduce fractional values of the structural dimensions, so instead we round the optimized dimensions of the stiffener model, and analysis it again.

Chapter 4

Integration shape and size optimization for radar mast

4.1 Original radar mast analysis

Radar mast is the primarily component in hull structure, it is usually located in at the top of ship and used for radar mounting, and it is highest component for ship. for good precision in detecting and target tracking, radar mast should be as steady as possible[100], the radar mast weight is heavier in hull structure, so it is necessary to carry out structure optimization and reduce weight for the radar mast. The original radar mast model is shown in the figure 4.1, whose thickness is 6mm and the materials used are mild steel.

Figure 4. 1 Original radar mast

According to new design requirement, two new stages are designed and used, the stage interval is determined, the main mast shape does not change, the new FEM model is shown in the figure 4.2.
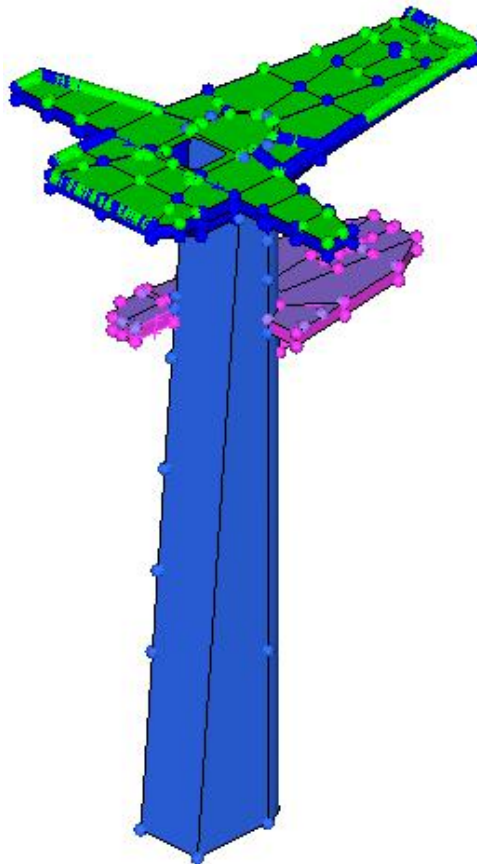

Figure 4. 2 FEM model

The load cases used in this chapter is the same as that used before. there are eight dynamic load cases should be considered on the voyage such as Sway, Surge, Roll load cases and so on which are represented in the form of acceleration, we combine and calculate the eight dynamic load cases in the longitudinal, transverse and vertical direction by the equivalent design wave, detailed load cases and combination method, please refer to [101].

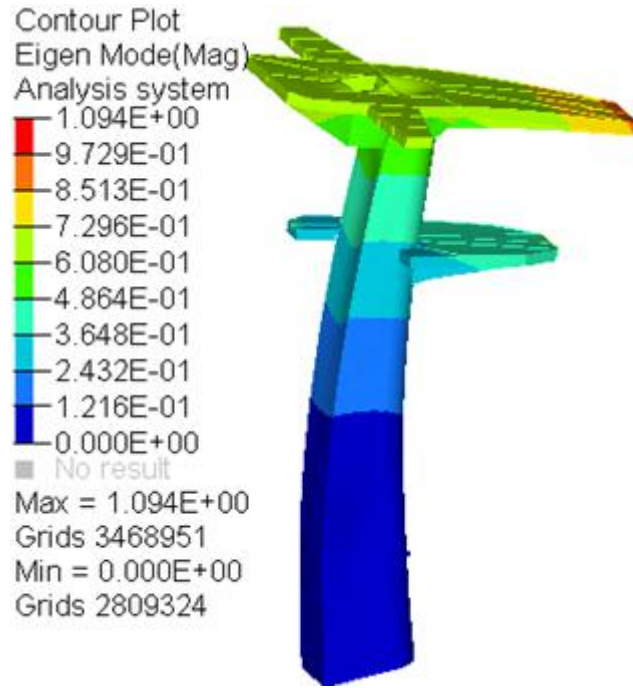Based on the above-mentioned loading state, the analysis results of radar mast without

wire are shown in the figure 4.2, which can be seen that the max suffered stress is

76Mpa. The max suffered stress is lower than the material of allowable stress. The

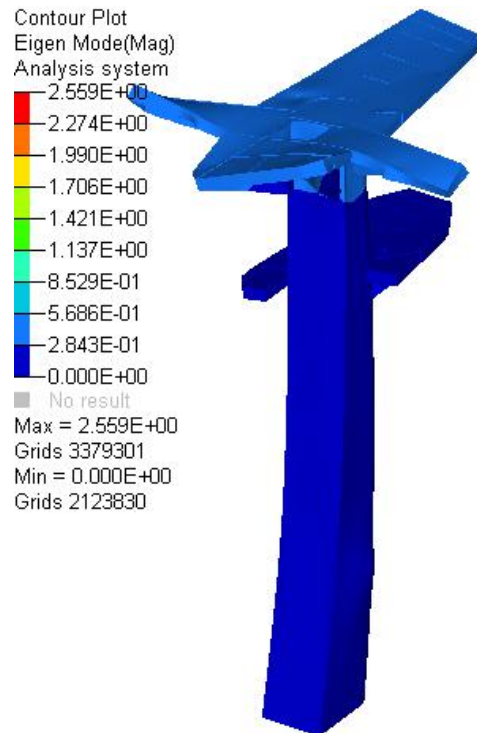Eigen frequency of radar mast and mode shape are shown as figure 4.3.
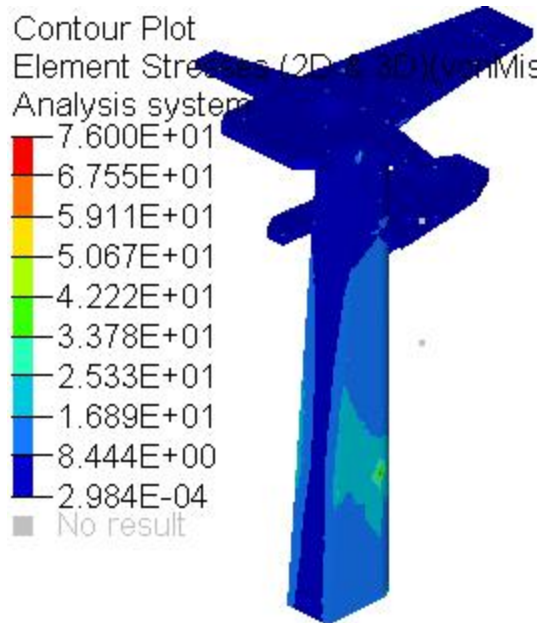
stress contour
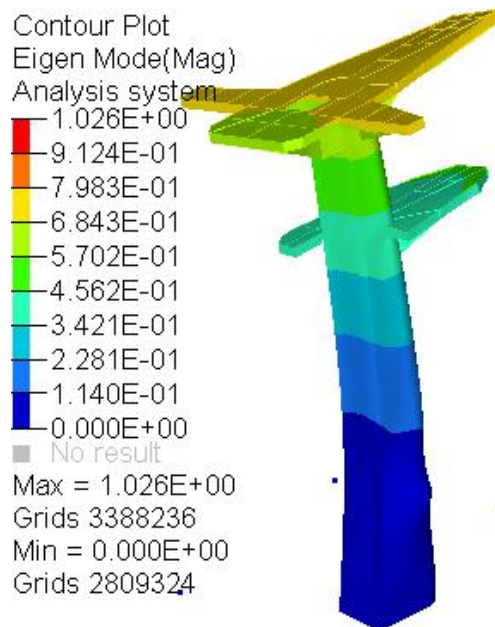
First-order

Second-order

Third-order

Figure 4. 3 The first three order modal shape

Order number	frequency	Mode shape
First	5.27 Hz	Left-right vibration
Second	6.64 Hz	Forth-back vibration
Third	10.26 Hz	torsion vibration

Table 4. 1 Radar mast eigen frequency

4.2 Integration optimization model

4.2.1 The mathematical model of integration optimization

This article aims to minimize radar mast weight, its thickness A and shape change X are design variables, allowable stress and first-order Eigen frequency are considered as constraint function, the optimization mathematical model can be shown in the follow equation,

Objection function: minimize M

Constraint function:

$$\omega_1 \geq 7\text{Hz}$$

$$\sigma_i \leq 310\text{MPa} \tag{4.1}$$

Design variable:

Radar mast thickness $3\text{mm} \leq A \leq 10\text{mm}$

Shape change   node displacement

In this equation, for obtaining higher Eigen frequency we set first-order frequency constraint value is 7Hz based on the radar mast with wire. The allowable stress is 310MPa.

4.2.2 Optimization process

The initial shape of radar mast is horseshoe shape (U-shaped), whose section parameters are shown in the follow figure 4.4.
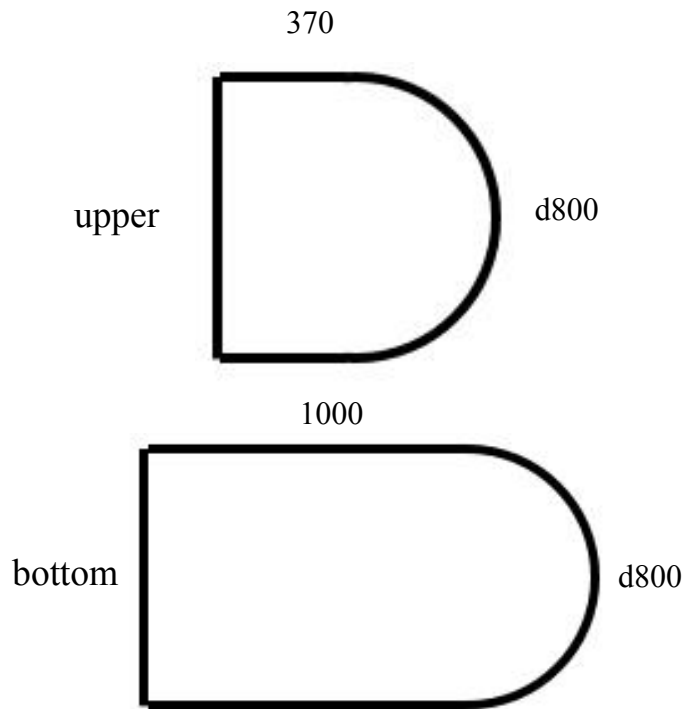

Figure 4. 4 Section parameter of original mast

According to the actual requirements of the shipbuilding company, we set first-order frequency as constraint function, making the first-order frequency over 7Hz after integration optimization. besides considering the productivity and aesthetics of the radar mast structure, manufacturing constraints should be added during optimization process, so symmetric manufacturing constraint is considered in this chapter. The objective for this optimization is to minimize the radar mast weight.

The load cases that adopt are based on the above section, then conducting the integrate of shape and size optimization. the iteration steps of radar mast weight are shown in the figure 4.5. the objective function tends to converge, the weight of radar mast

weight reaches the minimum.
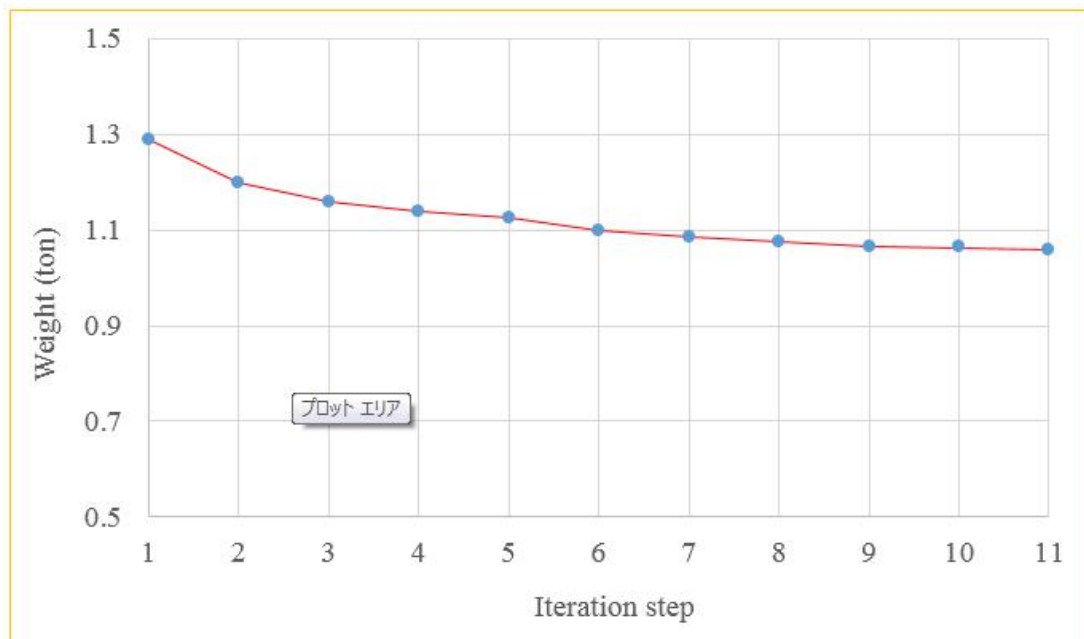
Figure 4. 5 Convergence history of radar mast weight

and the optimization results and mode shape are displayed in the following figure 4.6

and figure 4.7.
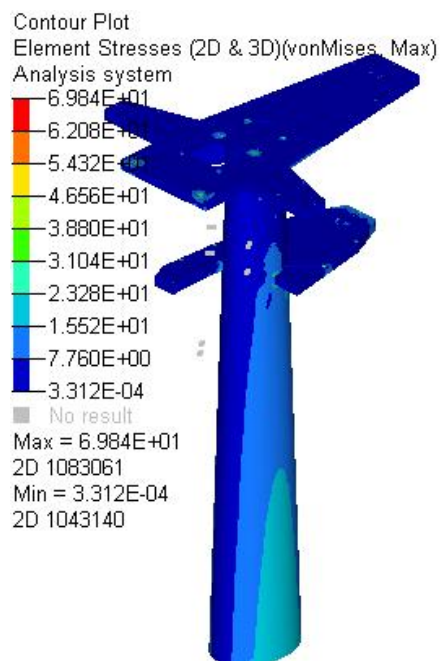
Figure 4. 6 Optimal results
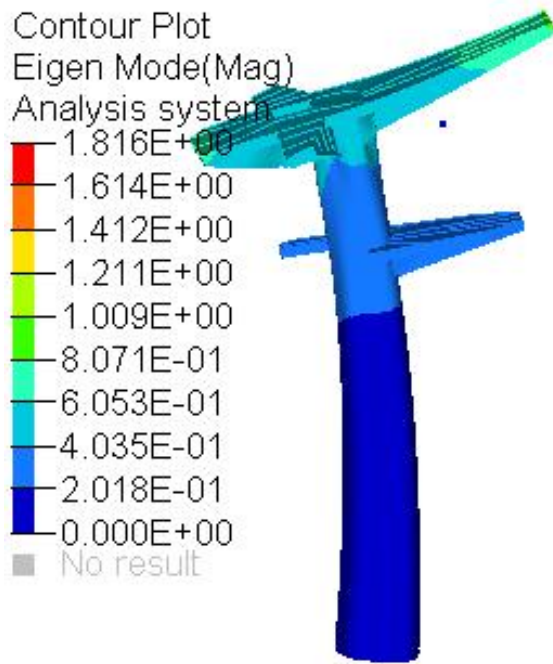
First-order
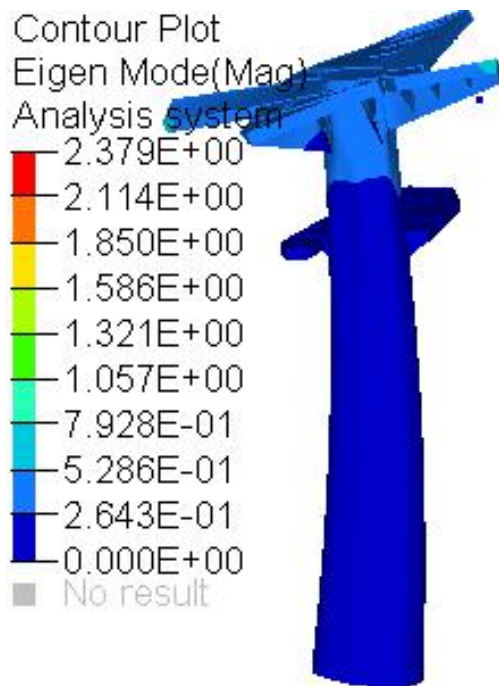
Second order
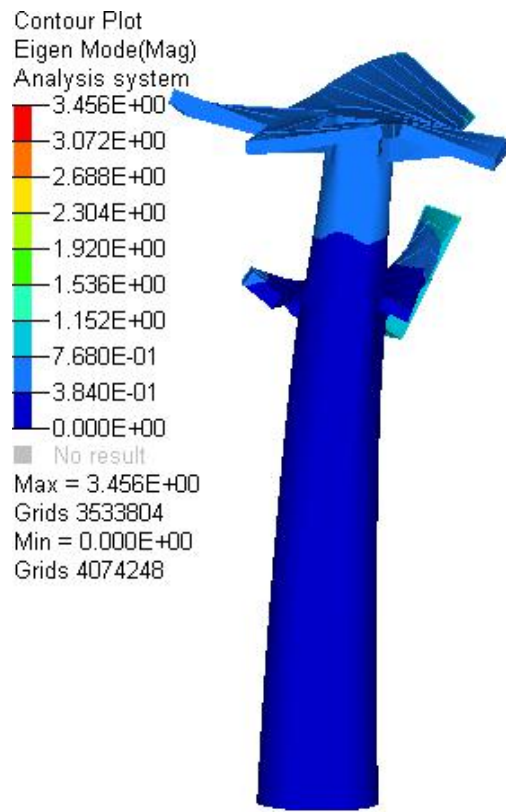
Third-order

Figure 4. 7 The first three order mode shape

Order number	frequency	Mode shape
First	7Hz	Forth-back vibration
Second	11.48 Hz	Left-right vibration
Third	15.02 Hz	Torsion vibration

Table 4. 2 Optimal Eigen frequency

Figure 4.6 shows that the max stress value which the radar mast suffered is 69.84Mpa, it is higher compared with original mast; the Eigen frequency value improved

compared with the original radar mast. The optimized radar mast thickness 5.4mm, and its weight is 1.06ton, the weight is reduced by 17.7%. But the optimized model is hard to manufacture, because the curve surface does not change uniformly, the detailed section shape as shown in figure 4.8.
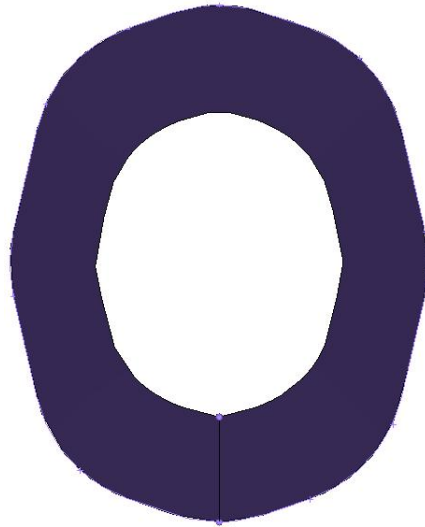
Figure 4. 8 Section shape

4.2.3 Alternatives optimization scheme

Based on the above optimization results and section shape, we can predict that the ideal radar mast should be tapered, the section of bottom is larger than the upper section. besides considering its machinability, the shape of radar mast should be able to change uniformly and smoothly.

Then two radar mast whose section are ellipse and circle respective are constructed, and the thickness is 5.4m based the above optimization results. the two predicted models are shown in the figure 4.9 and figure 4.10. We make sure that the section A and B can change proportionally during optimization process.
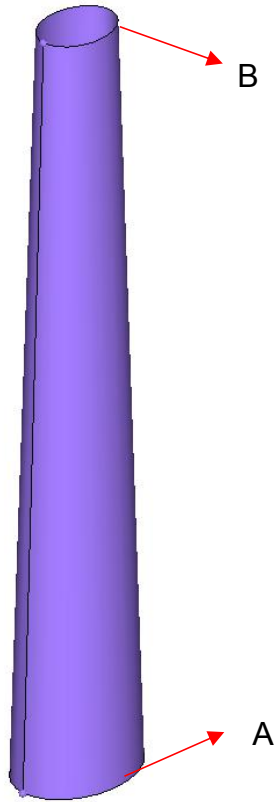
Figure 4. 9 Elliptical cylinders model

The elliptic equation of section A is as follow,

$$\frac{x^2}{696^2} + \frac{y^2}{532^2} = 1 \qquad (4.5)$$

The elliptic equation of section B is as follow,

$$\frac{x^2}{433^2} + \frac{y^2}{319^2} = 1 \qquad (4.6)$$
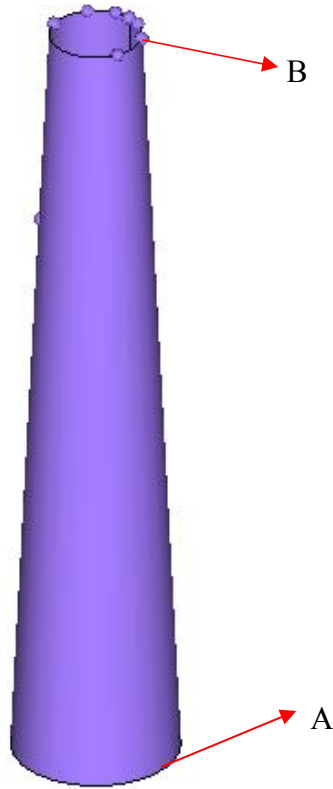
Figure 4. 10 Conical cylinders model

The circular equation of section A is as follow

$$x^2 + y^2 = 680^2 \qquad (4.7)$$

The circular equation of section B is as follow

$$x^2 + y^2 = 380^2 \qquad (4.8)$$

After the integration, the objective function of the two predicted model are all tend to converge, the convergence rate of the elliptical cylinders is faster than the conical cylinders model, the final optimal shape based on the predicted modes is consistent. the iteration steps of radar mast weight are shown in the follow figure. the objective function tends to converge, the weight of radar mast weight reaches the minimum.
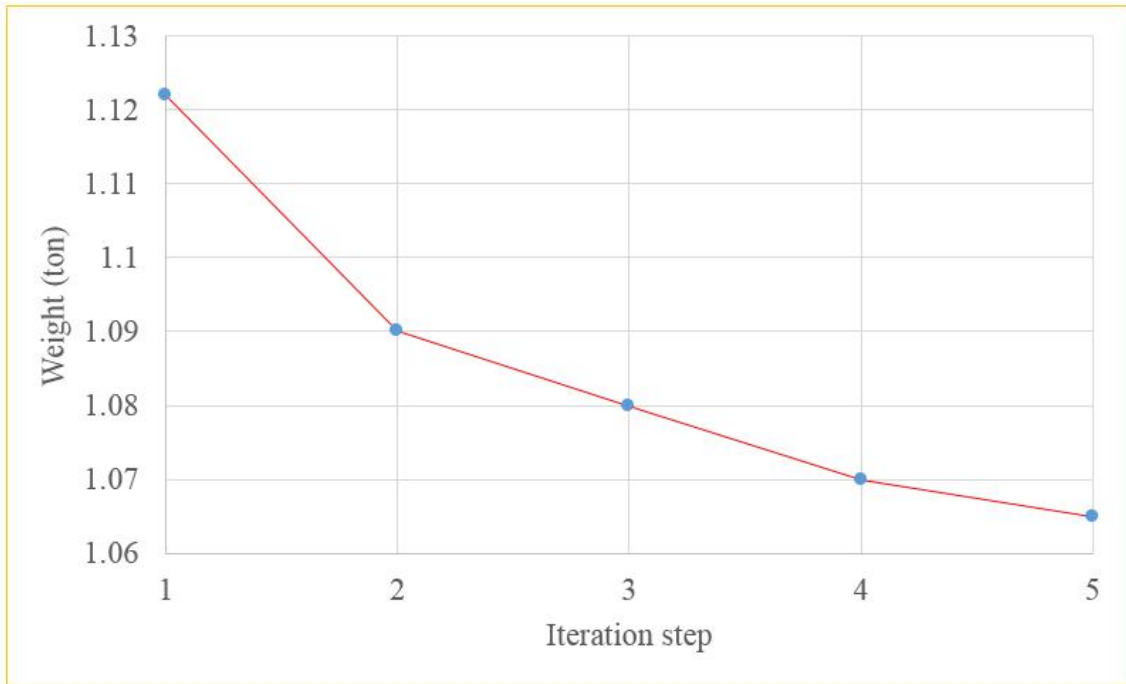
Figure 4. 11 Convergence history of elliptical cylinders model
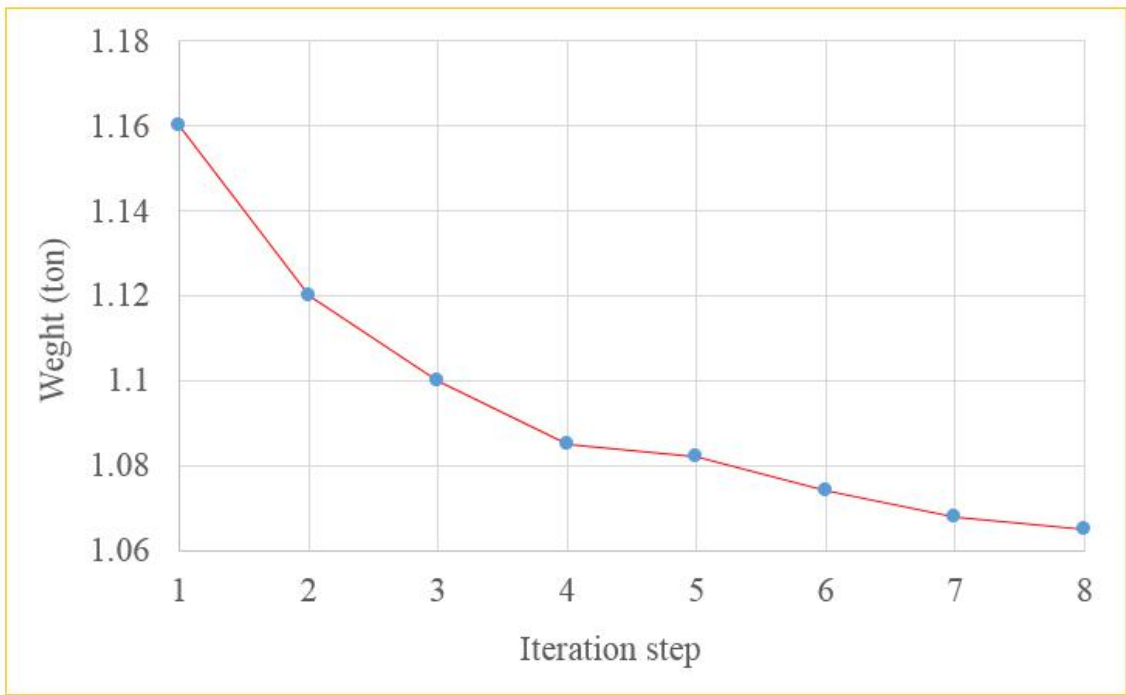
Figure 4. 12 Convergence history of conical cylinders model

The optimal shape of radar mast is shown in the following equation, and its thickness

is 5.4mm.

The elliptic equation of section A is as follow,

$$\frac{x^2}{695^2} + \frac{y^2}{530^2} = 1 \qquad (4.9)$$

The elliptic equation of section B is as follow,

$$\frac{x^2}{430^2} + \frac{y^2}{320^2} = 1 \qquad (4.10)$$

the final radar mast weight is 1.065ton.

4.3 Optimization results analysis

Based on optimization results, we construct the model and analysis it again, the analysis results are shown in the follow figure.
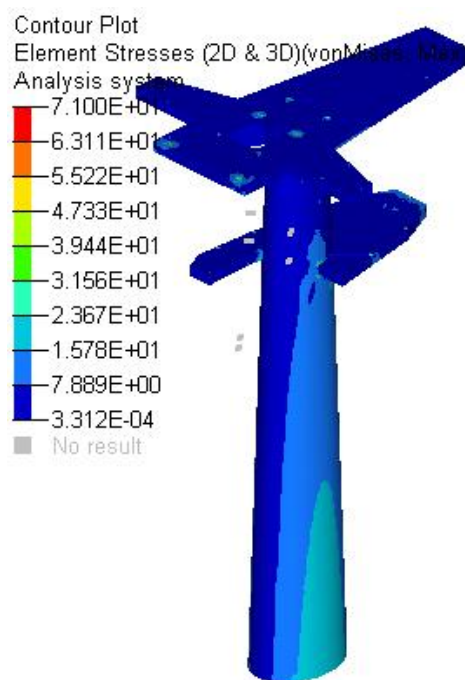
Figure 4. 13 Stress contours

Order number	frequency	Mode shape
First	7Hz	Forth-back vibration
Second	11.60 Hz	Left-right vibration
Third	15.5	Torsion vibration

Table 4. 3 Eigen frequency
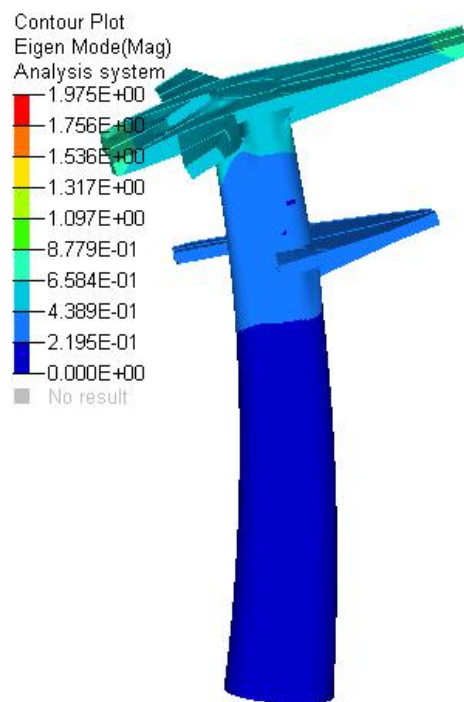
First-order
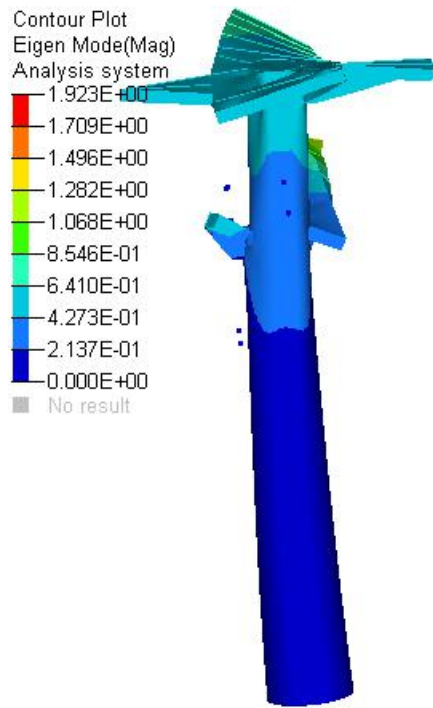
Second-order
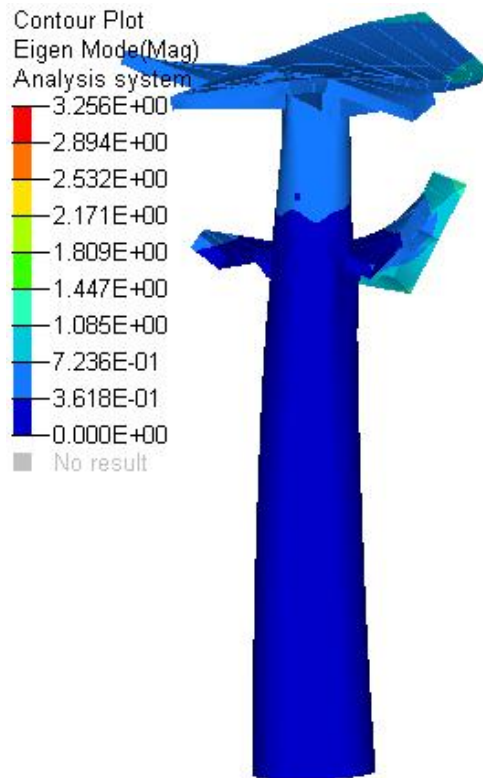
Third-order

Figure 4. 14 The first three order mode shape

Figure 4.13 shows the max stress value which the Elliptic cylinders radar mast suffered is 71Mpa separately, the stress value is lower than allowable stress, and the Eigen frequency are improved. The total weight reduces 17.31% compared with original radar mast.

4.4 Summary

The mechanical structure optimization of the radar mast was realized based on the integration shape and size optimization of the radar mast. In this paper, the load cases that the radar mast suffered, which is represented in the form of synthetic acceleration based on Common Structural Rules for Bulk Carriers and Oil Tankers (CSR-BC). Firstly, we get stress distribution and the first two modal shape by means of the finite element analysis (FEM) of the original radar mast for providing a theoretical basis for mechanism optimal design. Secondly, the mathematical model of the radar mast is built and calculated with the integration shape and size optimization and then the improving model come into being. Finally, the optimization of the radar mast is achieved under the condition of satisfying strength and the modal frequency is improved obviously.

It proves that the method of integration shape and sizing optimization is conducive to saving material, manpower, material resources and processing fees, which can also provide the effective reference to the lightweight research of the other ship structures.

Chapter 5

Concluding remarks

In this thesis, some main optimization methods (topology optimization, shape optimization, size optimization) combined with manufacturing process based on different algorithm are proposed to optimize the ship structures. This thesis mainly includes two parts, the first part is to apply the two-stage optimization method to find the best stiffener layout and size on the ship prow; the second part is to apply the integration shape and size optimization to optimize the radar mast. The main work that has been done and future work that needs to be done will be discussed in the following section.

In chapter 1, beginning with optimization applications in aerospace, shipbuilding and other field as the research background, these cases provide a reference for optimizing the ship structures in this thesis. after that, the different optimization methods used in this article are introduced in detail, the optimization theoretical basis for the ship structures in this thesis is found.

In chapter 2, the research object and the complex load cases it bears are discussed, and introduced how to connect these complicated load cases together by using the influence factors in detail. Later the two kinds of method about stiffener layout optimization is introduce, and the method of optimal thickness distribution method is applied to determine the stiffener layout in this thesis after comparing the advantages and disadvantages for these two methods. then taking multi-objective function as optimization objective function to generate stiffener based on some manufacturing

constraints, getting a reasonable material distribution (potential stiffener). actually, these potential stiffeners are hard to be manufactured, so we construct a regular stiffener based on optimization results and shipbuilding rules to replace the potential stiffener.

In chapter 3, we applied the size optimization method to optimize the stiffener size. Firstly, the section area of stiffener and plate thickness are selected as design variables based on some criterions, for making the optimization results reasonable and having practicability, each design variable has a range of values. besides the parameter relationships among these five design variables are set up which can avoid producing invalid dimensions. Secondly, the mathematical model of optimization is established, the minimum mass is set as the objective function based on buckling constraint. Lastly, an analysis model based on size optimization result is built, then finite element analysis method is conducted on this model, the analysis results prove that the size optimization is reasonable stage for ship prow.

In chapter 4, the mechanical structure optimization of the radar mast was realized based on the integration shape and size optimization method. Firstly, we provide an optimization theoretical evidence for radar mast based on analysis results. Secondly, we built the mathematical model base the integration shape and size optimization and then the improving model come into being. Finally, we analysis the new model again based the optimization results, the strength and eigen frequency meet the requirement.

To obtain even better structural performance, the following points should be considered in the future. the SIMP method uses a gradient optimization algorithm whose results converge toward a local optimum. Manufacturing constraints and appropriate optimization parameters are adopted in this study, which guide the research

closer to a global optimum. Hence, an appropriate algorithm should be explored that can avoid local convergence in 3D model optimization.

Reference

1. Revkin, A.C., *Obama speaks on climate at the U.N*, in *The New York Times*. 2009, The New York Times: New York.

2. Taylor, R., et al. *Detail part optimization on the F-35 joint strike fighter*. in *47th AIAA/ASME/ASCE/AHS/ASC Structures, Structural Dynamics, and Materials Conference 14th AIAA/ASME/AHS Adaptive Structures Conference 7th*. 2006.

3. Grihon, S., L. Krog, and D. Bassir, *Numerical optimization applied to structure sizing at AIRBUS: a multi-step process.* International Journal for Simulation and Multidisciplinary Design Optimization, 2009. **3**(4): p. 432-442.

4. Sekulski, Z., *Multi-objective topology and size optimization of high-speed vehicle-passenger catamaran structure by genetic algorithm.* Marine Structures, 2010. **23**(4): p. 405-433.

5. mingwen, S., *the structure optimization of ore carrier*. 2013, dalian universtiy of technology.

6. wang, z.l.r.h.r., *Topology optimization design of pure electric vehicle head based on frontal crash compatibility*. 2014.

7. Hu, h., *topolog optimization and sensitivity analysis for bus body structure.* Huazhong University of Science and Technology, 2006. **40**.

8. Tomlin, M. and J. Meyer. *Topology optimization of an additive layer manufactured (ALM) aerospace part*. in *Proceeding of the 7th Altair CAE technology conference*. 2011.

9. Wang, W., et al., *Cost-effective printing of 3D objects with skin-frame structures.* ACM Transactions on Graphics (TOG), 2013. **32**(6): p. 177.

10. Kavlie, D., et al., *Design optimization using a general nonlinear programming method.* European Shipbuilding, 1966. **15**(4): p. 57-62.

11. Xue, K., L. Li, and Q.H. Li. *Venation-Inspired Growth Technique for Stiffener Layout Design of Plate and Shell Structures*. in *Journal of Biomimetics, Biomaterials and Tissue Engineering*. 2013. Trans Tech Publ.

12. li, s., *Design principle for ship.* 1988.

13. yan., y.c.y.s.g., *submarine bulkhead optimization based on neural networks and genetic algorithms.* Shipbuilding of China, 2008. **49**(4): p. 81-87.

14. Sekulski, Z., *Multi-objective optimisation of ship hull structure by genetic algorithm with combined fitness function.* 2013. 515-524.

15. Ehlers, S., *A particle swarm algorithm-based optimization for high-strength steel structures.* Journal of Ship production and Design, 2012. **28**(1): p. 1-9.

16. zhang, c., *Structural optimization design and finite element analysis for trimaran*. 2012, Harbin Engineering University.

17. sijia, c., *Finite Element Analysis and Optimization of Key Structure on Huge firefighting ship*. 2014, dalian university of technology.

18. zhisheng, Z., *The FEA and Optimization of Ship Crane Boom*. 2016, jiangsu university.

19. Bendsoe, M.P. and O. Sigmund, *Topology optimization: theory, methods, and applications*. 2013: Springer Science & Business Media.

20. Bendsøe, M.P., *Optimal shape design as a material distribution problem*. Structural optimization, 1989. **1**(4): p. 193-202.

21. Schramm, U., et al. *Topology layout of structural designs and buckling*. in *10th AIAA/ISSMO Multidisciplinary Analysis and Optimization Conference*. 2004.

22. Liu, w., *topology optimization of an UAV landing gear structure* Mechanical Science and Technology, 2014. **33**(11): p. 1753-1757.

23. haitao cui, r.s., *genetic algorithm for topology optimization of continuum structure with stress and displacement constraints.* Chinese Journal of Aeronautics, 2005. **26**(1): p. 54-57.

24. zhong, h., *research on topology optimization of stiffened plates*. 2015, Nanjing University of Aeronautics and Astronautics.

25. Li, y., *Buckling analysis and optimization design of thin wall stiffened structure*. 2013, Beijing University of Technology

26. Rozvany, G.I., *Structural design via optimality criteria: the Prager approach to structural optimization*. Vol. 8. 2012: Springer Science & Business Media.

27. Belegundu, A.D. and J.S. Arora, *A study of mathematical programming methods for structural optimization. Part I: Theory.* International Journal for Numerical Methods in Engineering, 1985. **21**(9): p. 1583-1599.

28. Bendsøe, M.P. and O. Sigmund, *Material interpolation schemes in topology optimization.* Archive of applied mechanics, 1999. **69**(9-10): p. 635-654.

29. Sigmund, O. and K. Maute, *Topology optimization approaches.* Structural and Multidisciplinary Optimization, 2013. **48**(6): p. 1031-1055.

30. Bourdin, B., *Filters in topology optimization.* International Journal for Numerical Methods in Engineering, 2001. **50**(9): p. 2143-2158.

31. Rozvany, G., M. Zhou, and W. Gollub, *Continuum-type optimality criteria methods for large finite element systems with a displacement constraint. Part II.* Structural optimization, 1990. **2**(2): p. 77-104.

32. Diaz, A. and O. Sigmund, *Checkerboard patterns in layout optimization.* Structural

optimization, 1995. **10**(1): p. 40-45.

33. Sigmund, O. and J. Petersson, *Numerical instabilities in topology optimization: a survey on procedures dealing with checkerboards, mesh-dependencies and local minima.* Structural optimization, 1998. **16**(1): p. 68-75.

34. Matsui, K. and K. Terada, *Continuous approximation of material distribution for topology optimization.* International Journal for Numerical Methods in Engineering, 2004. **59**(14): p. 1925-1944.

35. tang, y., *Topology optimization design of continuum structures based on variable density method.* 2008, changan university.

36. Haber, R.B., C.S. Jog, and M.P. Bendsøe, *A new approach to variable-topology shape design using a constraint on perimeter.* Structural optimization, 1996. **11**(1-2): p. 1-12.

37. Petersson, J. and O. Sigmund, *Slope constrained topology optimization.* International Journal for Numerical Methods in Engineering, 1998. **41**(8): p. 1417-1434.

38. Kirsch, U., *Structural optimization : fundamentals and applications.* 1993: Springer-Verlag.

39. WANG, Y., *topology and size optimization designing for body in white of new energy vehicle.* 2012, Dalian university of technology.

40. Rosen, J.B., O.L. Mangasarian, and K. Ritter, *Nonlinear Programming: Proceedings of a Symposium Conducted by the Mathematics Research Center, the University of Wisconsin, Madison, May 4-6, 1970.* 2014: Elsevier.

41. Rao, J., *Advances in Aero Structures.* Procedia Engineering, 2016. **144**: p. 3-25.

42. Locatelli, D., *Optimization of supersonic aircraft wing-box using curvilinear SpaRibs.* 2012, Virginia Tech.

43. Lövgren, S. and E. Norberg, *Topology Optimization of Vehicle Body Structure for improved Ride & Handling.* 2011.

44. Rais-Rohani, M. and J. Lokits, *Reinforcement layout and sizing optimization of composite submarine sail structures.* Structural and Multidisciplinary Optimization, 2007. **34**(1): p. 75-90.

45. Qiu, W.Q., et al., *Structural design in cargo tank region for oil tankers based on topology optimization.* Ship & Boat, 2016.

46. Grujicic, M., et al., *Application of topology, size and shape optimization methods in polymer metal hybrid structural lightweight engineering.* Multidiscipline Modeling in Materials and Structures, 2008. **4**(4): p. 305-330.

47. Fan, W.-J. and N. Li, *Optimization Design Research on Stiffened Panels of*

Spaceborne Electronic Equipment [J]. Machine Design & Research, 2011. **2**: p. 016.

48. Chen, T. and C. Wang, *Topological and sizing optimization of reinforced ribs for a machining centre.* Engineering Optimization, 2008. **40**(1): p. 33-45.

49. Leiva, J., B. Watson, and I. Kosaka. *An Analyticall Bi-Directional Growth Parameterization to Obtain Optimal Castable Topology Designs.* in *10th AIAA/ISSMO Multidisciplinary Analysis and Optimization Conference.* 2004.

50. Zhu, J.-H., et al., *Structural design of aircraft skin stretch-forming die using topology optimization.* Journal of Computational and Applied Mathematics, 2013. **246**: p. 278-288.

51. Vatanabe, S.L., et al., *Topology optimization with manufacturing constraints: A unified projection-based approach.* Advances in Engineering Software, 2016. **100**: p. 97-112.

52. Sokolowski, J. and J.-P. Zolesio, *Introduction to shape optimization*, in *Introduction to Shape Optimization.* 1992, Springer. p. 5-12.

53. Sumner, R.W. and J. Popović. *Deformation transfer for triangle meshes.* in *ACM Transactions on Graphics (TOG).* 2004. ACM.

54. Samareh, J.A., *A survey of shape parameterization techniques.* 1999.

55. linzhen, Z., *production shape optimization based on MSC/NASTRAN* Machine Design & Research, 2006(10): p. 15-17.

56. yi, L., *structure optimization of motorcycle seat cushion bottom plate.* 2013, chongqing university.

57. cuidong, Y., *study of strcutural optimization method for launching canister of rocket launcher.* journal of north university of china (natural science edition), 2018. **39**(1): p. 61-68.

58. Zhen, Y., *The Structural Lightweight Design of Bridge Crane Girders Based on HyperWorks Shape Optimization.* Manufacturing Information Engineering of China, 2012. **41**: p. 43-48.

59. Jianguang, F., *Multi-Objective Shape Optimization of Body-in-White Based on Mesh Morphing Technology.* JOURNAL OF MECHANICAL ENGINEERING, 2012. **48**(24): p. 119-126.

60. cheng, g., *a new methods of structural shape optimization*, in *EPMESC.* 1992: dalian,china.

61. xiuli shen, w.w., *shape optimizaiton and application based on boundary element method.* journal of aerospace power, 1997. **12**(2): p. 113-116.

62. Jiajie, D., *Nose-shape optimization and simulation of projectiles penetrating into concrete target based on local interaction theory.* Explosion and Shock Waves, 2017.

$\mathbf{4}$(37): p. 611-620.

63.   zhang xiaozhen, s.r., *integration shape and sizing optimization of skyline clamp support.* Mechanical Design, 2016. $\mathbf{33}$(5): p. 40-43.

64.   Davidsson, P., J.A. Persson, and J. Holmgren. *On the integration of agent-based and mathematical optimization techniques.* in *KES International Symposium on Agent and Multi-Agent Systems: Technologies and Applications.* 2007. Springer.

65.   Wei, L., et al., *Truss optimization on shape and sizing with frequency constraints based on parallel genetic algorithm.* Structural and Multidisciplinary Optimization, 2011. $\mathbf{43}$(5): p. 665-682.

66.   Jiang, W.Z.W., *Optimal design for lightweight of structure of quayside container crane.* Journal of Mechanical Strength, 2012. $\mathbf{34}$: p. 615-620.

67.   wan, Y. *Application of Topology,sizing and Shape Optimization Methods to Optimal Design of Aircraft Components.* in *Altair 2012 conference*

68.   Hua, Z., *Parallel Collaborative Optimization Method of the Size andShape of Air Vehicle Structure.* 2012, Nanjing University of Aeronautics and Astronautics.

69.   Safari, A., et al., *Role of Gas-Fuelled Solutions in Support of Future Sustainable Energy World: Part II: Case Studies*, in *Sustainable Energy Technology and Policies.* 2018, Springer. p. 35-86.

70.   IACS, *Common Structural Rules for Bulk Carriers and Oil Tankers.* 2017.

71.   DOM, W., *Automatic design of optimal structures.* J. de mechanjque (Eur. J. Mech.), 1964. $\mathbf{3}$: p. 25-52.

72.   Oberndorfer, J.M., W. Achtziger, and H.R. Hörnlein, *Two approaches for truss topology optimization: a comparison for practical use.* Structural optimization, 1996. $\mathbf{11}$(3-4): p. 137-144.

73.   LIU, Q.-m. and L.-b. YAN, *Optimal designing method for reinforced ribs of sheet metal structure based on yielding criterion of fringe fibre.* Journal of Machine Design, 2007. $\mathbf{4}$: p. 010.

74.   Krog, L., et al. *Topology optimisation of aircraft wing box ribs.* in *10th AIAA/ISSMO multidisciplinary analysis and optimization conference.* 2004.

75.   Wang, Q., Z. Lu, and C. Zhou, *New topology optimization method for wing leading-edge ribs.* Journal of Aircraft, 2011. $\mathbf{48}$(5): p. 1741-1748.

76.   Locatelli, et al., *Wing-box weight optimization using curvilinear spars and ribs (SpaRibs).* J Aircr, 2011. $\mathbf{48}$(5): p. 1671-1684.

77.   Maute, K. and M. Allen, *Conceptual design of aeroelastic structures by topology optimization.* Struct Multidiscipl Optim, ,2004. $\mathbf{27}$(1): p. 27-42.

78.   Ding, X. and K. Yamazaki, *Adaptive growth technique of stiffener layout pattern*

for plate and shell structures to achieve minimum compliance. Eng Opti, 2005. **37**(3): p. 259-276.

79.   Bojczuk, D. and W. Szteleblak, *Optimization of layout and shape of stiffeners in 2D structures.* Comput Struct, 2008. **86**(13): p. 1436-1446.

80.   Ishii, K. and S. Aomura, *Topology optimization for the extruded three dimensional structure with constant cross section.* JSME INT J A SOLID M, ,2004. **47**(2): p. 198-206.

81.   Liu, S., et al., *H-DGTP—a Heaviside-function based directional growth topology parameterization for design optimization of stiffener layout and height of thin-walled structures.* Struct Multidiscipl Optim, ,2015. **52**(5): p. 903-913.

82.   Cheng, K.-T. and N. Olhoff, *An investigation concerning optimal design of solid elastic plates.* International Journal of Solids and Structures, 1981. **17**(3): p. 305-323.

83.   Rong, J., Y. Xie, and X. Yang, *An improved method for evolutionary structural optimisation against buckling.* Computers & Structures, 2001. **79**(3): p. 253-263.

84.   Wenjie FAN, J.X., *loading arm structure topology optimization based on BESO method.* Transactions of The Chinese Society of Agricultural 2006(11): p. 24-27.

85.   Fan, W.-J., Z.-J. Fan, and R.-Y. Su, *Research on multi-objective topology optimization on bus chassis frame.* Chin. J. Mech. Eng, 2008. **19**(12): p. 1505-1508.

86.   Liu, L., Y. Xin, and W. Wang, *Multi-objective topology optimization for an off-road vehicle frame based on compromise programming.* Mech Sci Technol Aerosp Eng, 2011. **30**(3): p. 382-385.

87.   Jiang, J., et al., *Multi-objective topology optimization of a mining dump truck frame.* Zhongguo Jixie Gongcheng(China Mechanical Engineering), 2013. **24**(8): p. 1028-1032.

88.   Jiang, C., et al., *The U-type Platform Multi-objective Topology Optimization Research*, in *4th International Conference on Computer, Mechatronics, Control and Electronic Engineering.* 2015.

89.   Ma, Z.-D., N. Kikuchi, and H.-C. Cheng, *Topological design for vibrating structures.* Computer methods in applied mechanics and engineering, 1995. **121**(1-4): p. 259-280.

90.   Min, S., S. Nishiwaki, and N. Kikuchi, *Unified topology design of static and vibrating structures using multiobjective optimization.* Computers & Structures, 2000. **75**(1): p. 93-116.

91.   Rao, S. and T. Freiheit, *A modified game theory approach to multiobjective optimization.* Journal of Mechanical Design, 1991. **113**(3): p. 286-291.

92.   Nocedal, J. and S. Wright, *Numerical optimization.* ,2006: Springer Science & Business Media.

93.   CHEN, H., *Modal analysis and topology optimization for the cab of heavy duty commercial vehicle.* 2009, JIlin university.

94.   Jiqing, L.J.L.F.C., *New Technology of Lightweight and Steel-aluminum Hybrid Structure Car Body [J].* Chinese Journal of Mechanical Engineering, 2008. **6**: p. 006.

95.   Dugré, A. and A. Vadean, *Challenges of using topology optimization for the design of pressurized stiffened panels.* Structural and Multidisciplinary Optimization, 2016. **53**(2): p. 303-320.

96.   MEI, L., *staic analysis of hat stiffeners on the composite ship.* ship science and technology, 2015(4): p. 41-46.

97.   Han, X., *structure optimization of comosite hat-stiffened panel.* 2009, Nanjing University of Aeronautics and Astronautics 2009.

98.   Veritas, D.N., *Hull structural design ships with length 100 metres and above.* DNV Rules for Classification of Ships, 2009.

99.   Fei, W., *topology and size optimization research on metro vehicle bogie framework of type B.* 2012, beijing jiaotong university.

100.   WeiKang, Z.W.J., *OPTIMAL DESIGN FOR LIGHTWEIGHT OF STRUCTURE OF QUAYSIDE CONTAINER CRANE [J].* Journal of Mechanical Strength, 2012. **4**: p. 027.

101.   Society, I.A.C., ed. *Commom Strutural Rules for Bulk Carriers and Oil Tankers.* 2015. 157-190.

Publications List

1. Zhijun Liu, Shingo Cho, Akihiro Takezawa, Xiaopeng Zhang, Mitsuru Kitamura. Two-stage layout–size optimization method for prow stiffeners. International Journal of Naval Architecture and Ocean Engineering. in press.

2. Zhijun Liu, Akihiro Takezawa, Xiaopeng Zhang, Mitsuru Kitamura. Integration shape and size optimization of ship structure. Asian Congress of Structural and Multidisciplinary Optimization 2018.